Unemployment Crises

Nicolas Petrosky-Nadeau* FRB San Franciso

Lu Zhang† Ohio State and NBER

December 2018‡

Abstract

A search model of equilibrium unemployment, calibrated to the postwar sample, potentially explains the unemployment crisis in the Great Depression. The limited responses of wages from credible bargaining to aggregate conditions, along with matching frictions, cause the unemployment rates to rise sharply in recessions but to decline only gradually in booms. The frequency and severity of the crises in the model are quantitatively consistent with U.S. historical data. However, when we feed the measured labor productivity into the model, its unemployment crisis is less persistent than that in the 1930s.

JEL Classification: E24, E32, J63, J64.

Keywords: Search and matching, unemployment crises, the Great Depression, the unemployment volatility, nonlinear impulse response functions

*Federal Reserve Bank of San Francisco, 101 Market Street, San Francisco CA 94105. Tel: (415) 974-2740. E-mail: Nicolas.Petrosky-Nadeau@sf.frb.org.

†Fisher College of Business, The Ohio State University, 760A Fisher Hall, 2100 Neil Avenue, Columbus OH 43210; and NBER. Tel: (614) 292-8644. E-mail: zhanglu@fisher.osu.edu.

‡We are grateful to Hang Bai, Andrew Chen, Daniele Coen-Pirani, Steven Davis, Mariacristina De Nardi, Paul Evans, Wouter Den Haan, Bob Hall, Dale Mortensen, Morten Ravn, Paulina Restrepo-Echavarria, Robert Shimer, Etienne Wasmer, Randall Wright, Rafael Lopez de Melo, and other seminar participants at Federal Reserve Bank of San Francisco, Northwestern University, The Ohio State University, University of Georgia, University of California at Irvine, University of California at Los Angeles, Université du Québec à Montréal, University of California at Berkeley, University of California at Santa Cruz, University of Southern California, Kiel Institute, Sciences Po Paris, University College London, University of Montreal, University of Texas at Austin, and University of Edinburgh, as well as the 19th International Conference on Computing in Economics and Finance hosted by the Society for Computational Economics, the 2013 North American Summer Meeting of the Econometric Society, the Southwest Search and Matching workshop at University of Colorado at Boulder, the 2014 meeting of the Canadian Economic Association, Oslo New Developments in Business Cycle Analysis conference, and the 2014 NBER Summer Institute Macro Perspectives Workshop for helpful comments. Rui Gong and Patrick Kiernan have provided exemplary research assistance. Nicolas Petrosky-Nadeau thanks Stanford Institute for Economic Policy Research and the Hoover Institution at Stanford University for their hospitality. The views expressed in this paper are those of the authors and do not necessarily reflect the position of the Federal Reserve Bank of San Francisco or the Federal Reserve System.

1 Introduction

The unemployment rates in the United States exhibit extraordinary dynamics in the 1930s, known as the Great Depression. From January 1931 to December 1939, the average civilian unemployment rate is 14.77%, and the highest unemployment rate hits 25.54% in July 1932. In contrast, such large dynamics are absent in the postwar sample. From January 1951 to December 2017, the mean unemployment rate is only 5.83%, and the maximum never exceeds 11%. We fit a three-state Markov chain on the historical series via maximum likelihood. Identifying months in which civilian unemployment rates are above 15% as the crisis state, we estimate the unconditional probability of an unemployment crisis to be 2.93% and its persistence (the probability of a crisis next period conditional on a crisis in the current period) to be 91.11% in the 1890–2017 sample.

This paper asks whether a search model of equilibrium unemployment, when calibrated to the mean and volatility of unemployment in the postwar sample, can explain the large unemployment dynamics in the Great Depression. Perhaps surprisingly, the answer is affirmative, quantitatively.

In the model, unemployed workers search for vacancies posted by a representative firm. A matching function takes vacancies and unemployed workers as inputs to produce the number of new hires in the labor market. Because of the congestion effect arising from matching frictions, the vacancy filling rate decreases with the tightness of the labor market (the ratio of the number of vacancies over the number of unemployed workers). Deviating from the standard wage determination from a Nash bargaining game, we derive the equilibrium wage from a credible bargaining game per Hall and Milgrom (2008). In this setup, both parties make alternating offers that can be accepted, rejected to make a counteroffer, or rejected to take outside options. Relative to the Nash wage, the credible bargaining wage is more insulated from aggregate conditions in the labor market.

Our key insight is that the search model is capable of endogenizing unemployment crises as in the Great Depression, even though the exogenous driving force is a standard first-order autoregressive process with homoscedastic lognormal shocks. When calibrated to the mean of 5.83% and

the volatility of 0.126 of the unemployment rates in the postwar sample, the model implies the persistence of the crisis state to be 91.8% and its unconditional probability 4.77%, both of which are close to 91.1% and 2.93% in the historical data, respectively. The unemployment dynamics in the model are large and highly nonlinear. In recessions, the unemployment rates rise drastically, only to decline gradually in booms. The empirical stationary distribution is highly skewed with a long right tail. The skewness in the model is 2.06 (with a cross-simulation standard deviation of 0.59) and is close to 2.29 in the historical data. However, the kurtosis in the model is 7.9 (with a cross-simulation standard deviation of 3.62) and is lower than 11.12 in the data.

We shed new light on the second moments of the labor market. The volatility of civilian unemployment rates is 0.258 in the 1890–2017 sample, more than doubling the volatility of 0.126 in the post-1951 sample. In addition, drawing from a variety of rarely used data sources, we compile a historical vacancy rate series from January 1919 to December 2017 as well as a labor productivity series that dates back to January 1890. The volatility of the vacancy rates is 0.172 in the long sample, which is only somewhat higher than 0.135 in the postwar sample. However, the historical volatility of the labor market tightness to be 0.379, which is substantially higher than 0.256 in the postwar sample. The U.S. Beveridge curve is flatter in the long sample than in the postwar sample, as the unemployment-vacancy correlations are -0.79 and -0.92 across the two samples, respectively. The model predicts the volatility of the market tightness to be 0.3 in crises and 0.27 in normal periods, as well as a flatter Beveridge curve in crises. However, calibrated to the postwar volatility of the labor productivity, the model predicts an unemployment volatility of only 0.156 in crises.

Credible bargaining plays a key role in driving our results. With bargaining parties making alternating offers instead of taking outside options in the credible bargaining game, the equilibrium wage is insulated from conditions in the labor market. In addition, the congestion externality from matching frictions also plays a role. In recessions many unemployed workers compete for a small pool of vacancies. An extra vacancy is quickly filled, and the vacancy filling rate hardly increases. As a result, the marginal cost of hiring declines very slowly, giving rise to downward rigidity (Petrosky-

Nadeau, Zhang, and Kuehn 2018). When a large negative shock hits the labor productivity, output falls, but profits plummet more, because the wage is insensitive to aggregate conditions. To make things worse, the marginal cost of hiring fails to decline to offset the impact of falling profits on the hiring incentives. Consequently, unemployment rises drastically, giving rise to crises.

Comparative statics show that the probability of bargaining breakdown and the firm's delaying cost during each round of alternating offers, which are two key parameters in the credible bargaining game, are quantitatively important for the crisis dynamics. A higher probability of breakdown, in which both parties take outside options, brings the credible bargaining closer to the Nash bargaining, and makes the equilibrium wage more responsive to labor market conditions. As such, the crisis dynamics are dampened. In contrast, a higher delaying cost makes the equilibrium wage more insulated from labor market conditions, strengthening the crisis dynamics.

Finally, we feed the labor productivity data in the Great Depression into the model, compute the predicted output, unemployment, and market tightness series, and compare them with those in the data. The model does a good job in tracking the large output drop in 1933. The model also predicts that the unemployment rate reaches over 35%, which is even higher than the civilian unemployment rate of 25.5% but close to the private nonfarm unemployment rate in 1933. However, the high unemployment rates in the model are less persistent than the observed unemployment rates in the 1930s.

Our work makes three contributions. First, the macro labor literature has mostly studied the second moments of the labor market, but not higher moments (Shimer 2005).[1] Going beyond the second moments, we highlight the nonlinear dynamics of the search model and demonstrate its potential to explain the unemployment crisis in the Great Depression. We also compile the historical series of civilian and private nonfarm unemployment rates, vacancy rates, and labor productivity

[1]The theoretical foundations for the search model are provided by Diamond (1982), Mortensen (1982), and Pissarides (1985). Shimer (2005) shows that the unemployment volatility in the search model is too low relative to that in the data. A large subsequent literature has developed to address the volatility puzzle. Hall (2005) and Hall and Milgrom (2008) show how wage stickiness, which satisfies the condition that no worker-firm pair has any unexploited opportunity for mutual gain, increases labor market volatilities. Mortensen and Nagypál (2007) and Pissarides (2009) show that the fixed recruiting cost can explain the volatility puzzle. Hagedorn and Manovskii (2008) show that a calibration with small profits and a low bargaining power for the workers can produce realistic volatilities. Petrosky-Nadeau and Wasmer (2013) show how incorporating financial frictions can generate higher labor market volatilities.

from January 1890 onward that have rarely been used in the prior macro labor literature.

Second, our work is related to the Great Depression literature. Using the stochastic growth model, Cole and Ohanian (2004) and Ohanian (2009) quantify important deviations from the neoclassical equilibrium conditions in the labor market in the 1930s. Their results emphasize the impact of wage rigidity and other frictions in the labor market. We bring historical data on unemployment and vacancy rates to the scope of analysis. More important, the search model seems a better fit for studying labor market frictions. As such, we view our work as highly complementary to theirs.

Finally, we contribute to the disasters literature in economics and finance (Rietz 1988; Barro 2006; Gourio 2012). Prior studies mostly specify disasters exogenously, but our crises are entirely endogenous, despite calibrating to the postwar sample. Petrosky-Nadeau, Zhang, and Kuehn (2018) calibrate a baseline search model with the Nash wage to the output and consumption disasters in the Barro and Ursua (2008) cross-country panel. We instead focus on the crises in the labor market. We also move beyond the Nash bargaining to the Hall and Milgrom (2008) credible bargaining, which seems a more appropriate modeling choice for the wages in the Great Depression.

Section 2 documents the historical facts of the U.S. labor market. Section 3 describes the model with credible bargaining. Section 4 presents the quantitative results. Finally, Section 5 concludes.

2 U.S. Labor Market: Historical Facts

We compile the historical series of unemployment rates, vacancy rates, and labor productivity, and describe their time series properties in Section 2.1. The series for unemployment rates and labor productivity date back to January 1890, and the series for vacancy rates to January 1919. We calculate labor market moments, including volatilities and tail probabilities, in Section 2.2.

2.1 Sample Construction and Descriptive Properties

This subsection discusses important conceptual issues on the sample construction. Appendix A describes in detail our data and step-by-step procedures that we use to compile our historical series.

2.1.1 Unemployment Rates

From January 1948 to December 2017, we use civilian unemployment rates (seasonally adjusted) from Bureau of Labor Statistics (BLS) from U.S. Department of Labor. No adjustment is necessary.

Prior to 1948, we rely on Weir (1992), who in turn builds on Lebergott (1964). Weir provides an annual series of civilian unemployment rates that date back to 1890. We accept Weir's annual values, but seek to temporally disaggregate his series to the monthly frequency. For this purpose, we use the Denton (1971) proportional first difference procedure. The key issue is then what sub-annual series to use as the monthly indicators in the Denton procedure.

From January 1930 to December 1947, we use the unemployment rates drawn from NBER macrohistory files (chapter 8: Income and employment): (i) January 1930–February 1940, series m08292a, seasonally adjusted; (ii) March 1940–December 1946, series m08292b, seasonally adjusted; and (iii) January 1947–December 1947, series m08292c, not seasonally adjusted. We pass the entire series m08292c from January 1947 to December 1966 through the X12 seasonal adjustment program from U.S. Census Bureau and take the adjusted monthly observations in 1947. We impose the monthly average of the interpolated series in a given year to equal that year's annual value in Weir.

From January 1890 to December 1929, we need to use a different monthly indicator series, as the NBER series m08292a starts only in April 1929. Bai (2016) documents that the unemployment rates and the yield spread between Moody's Baa- and Aaa-rated corporate bonds have a high correlation of 0.81 from April 1929 to March 2015. As such, we construct a monthly indicator series of the yield spread: (i) NBER macrohistory series m13019 (January 1857–January 1937, American railroad bond yields, high grade); (ii) NBER macrohistory series m13019a (January 1857–December 1934, U.S. railroad bond yields); and (iii) Moody's Baa- and Aaa-rated corporate bond yields from Federal Reserve Bank of St. Louis (January 1919–December 2017). We quarterly splice the railroad yield spread (series m13019a minus series m13019) to the Moody's yield spread series (Baa minus Aaa) in the first quarter of 1919. Specifically, we rescale the railroad spread series so that its monthly aver-

age in the first quarter of 1919 equals that of the Moody's series in the same quarter. We then take the values of the concatenated series from January 1890 to December 1929 as the monthly indicator.

Weir (1992) sides with Darby (1976) in counting all government emergency workers as employed, a practice that is more consistent with the modern definition of civilian unemployment. To address Lebergott's (1964) concern that counting these workers as unemployed more accurately depicts the failure of the private economy, Weir provides a separate series for private nonfarm unemployment rates. To calculate the alternative unemployment rates, Weir subtracts farm and government employment from both the civilian labor force and civilian employment. Following Weir, we also construct a historical series of private nonfarm unemployment rates from January 1890 onward.

From January 1890 to December 1947, we use the Denton (1971) proportional first difference procedure to temporally disaggregate Weir's (1992) annual private nonfarm unemployment rates series to monthly. The monthly indicators are the spliced yield spread series from January 1890 to December 1929 and the NBER macrohistory unemployment rates from January 1930 onward (the same indicators that we use to interpolate Weir's civilian unemployment rates).

From January 1948 to December 2017, we calculate private nonfarm unemployment rates as: (Civilian labor force − civilian employment)/(civilian labor force − (farm employment + government employment)). In the numerator, both terms should deduct the sum of farm and government employment to yield private nonfarm labor force and private nonfarm employment, respectively. As such, the numerator equals civilian unemployment, which we obtain from the Current Population Survey (CPS). In the denominator, we back out the sum of farm and government employment as the CPS civilian employment minus the private nonfarm employment from the Current Employment Statistics (CES) released by BLS. While we acknowledge the important differences between CPS and CES (Bowler and Morisi 2006), Weir also uses CES-based government employment.

Figure 1 plots the U.S. monthly civilian and private nonfarm unemployment rates from 1890 to 2017. The most striking feature of the series is the extraordinary high unemployment rates in the

1930s, known as the Great Depression. The mean civilian unemployment rate is 6.27% in the full sample, 6.76% in the pre-1951 sample, and 5.83% in the post-1951 sample. The median is 5.54% in the full sample, which is close to 5.6% in the post-1951 sample. However, the skewness is 2.29, and kurtosis 11.12 in the full sample, which are substantially higher than 0.6 and 3.08, respectively, in the post-1951 sample. In particular, from January 1931 to December 1939, its average is 14.77%, and the highest civilian unemployment rate reaches 25.54% in July 1932.

The contrast between the full and post-1951 samples is also stark for private nonfarm unemployment rates. The full sample mean is 8.88%, 10.31% in the pre-1951 sample, and 7.59% in the post-1951 sample. The median is 7.72% in the full sample, which is close to 7.3% in the post-1951 sample. However, the skewness is 2.15, and kurtosis 9.61 in the full sample, which are substantially higher than 0.59 and 2.93 in the post-1951 sample, respectively. In particular, its 1931–1939 average is 21.21%, and the highest private nonfarm unemployment rate hits 35.46% in July 1932. Such large unemployment dynamics are absent in the postwar sample.

2.1.2 Vacancy Rates

We construct a historical series for vacancy rates from January 1919 to December 2017. From December 2000 onward, we obtain the seasonally adjusted total nonfarm job openings from the Job Openings and Labor Turnover Survey (JOLTS) at BLS. This series contains government job openings. Because the series of government vacancies is not separately available prior to JOLTS, we use total nonfarm job openings throughout the sample to be consistent.

From January 1995 to November 2000, we use the seasonally adjusted composite print and online help-wanted index from Barnichon (2010), obtained from Regies Barnichon's Web site. We quarterly splice the Barnichon series to the JOLTS series in the first quarter of 2001. From January 1960 to December 1994, we use the seasonally adjusted help-wanted advertising index from the Conference Board. We quarterly splice the Conference Board series in the first quarter of 1995 to the Barnichon series (already spliced to the JOLTS series in the first quarter of 2001).

From January 1919 to December 1950, we use the Metropolitan Life Insurance company (MetLife) help-wanted advertising index from NBER macrohistory files (series m08082a, January 1919–August 1960, not seasonally adjusted). The Conference Board series is similar, statistically and methodologically, to the MetLife series (Preston 1977). We seasonally adjust the MetLife series with the X12 program, and quarterly splice the seasonally adjusted MetLife series in the first quarter of 1951 to the Conference Board series (already spliced to the rescaled Barnichon series).

To convert the vacancy series into vacancy rates, we need to construct a series of the civilian labor force. From January 1948 to December 2017, we utilize the monthly civilian labor force over 16 years of age from the CPS (seasonally adjusted, number in thousands). No adjustment is necessary. From January 1890 to December 1947, we start with Weir's (1992) annual civilian labor force series (1890–1990, 14 years and older through 1946, 16 years and older afterward). We use the Denton proportional first difference procedure to interpolate Weir's annual series to monthly, with a vector of ones as the monthly indicator. We then annual splice the interpolated Weir series to the CPS series in the year 1948. Finally, dividing the vacancy series by the labor force series yields the historical series of vacancy rates from January 1919 to December 2017.

Figure 2 plots the constructed U.S. monthly job openings, civilian labor force, vacancy rates, and labor market tightness (vacancy rates divided by civilian unemployment rates) from January 1919 to December 2017. The average vacancy rate is 3.12% in the full sample, 2.87% prior to January 1951, and 3.23% afterward. The pre-1951 vacancy rates are clearly more volatile. In particular, the early 1920s feature surprisingly high levels of job openings and vacancy rates. Their vacancy rates are even higher than those during the second World War. This evidence should be interpreted with caution. The MetLife help-wanted index was initiated in 1927 by William A. Berridge. Past issues of print newspapers were collected to gather data back to 1919, but only one-third of the newspapers in his index provided historical data in 1927 (Berridge 1929, 1961). Motivated by this concern, Zagorsky (1998), for example, builds on the MetLife series only from January 1923 onward. The average labor market tightness is 0.72 in the full sample, 0.91 prior to 1951, and 0.62 afterward.

The pre-1951 sample is clearly more volatility. In particular, the second World War is an important outlier in that the labor market tightness reaches its highest level of 6.89 in October 1944.

Figure 3 reports the U.S. historical Beveridge curve by plotting the vacancy rates against civilian unemployment rates from January 1919 to December 2017. Several patterns emerge. First, the scatter points display a clear convex shape, a pattern consistent with the congestion externality due to matching frictions in the labor market. Second, the pre-1951 sample shows more dramatic movements in the unemployment and vacancy rates than the post-1951 sample. In particular, when the unemployment rates exceed 20% in the Great Depression, the vacancy rates are below 1%. When the unemployment rates are below 1% during the second World War, the vacancy rates hit high levels of above 6%. In contrast, such large movements are absent from the post-1951 sample, in which the unemployment rates barely move above 10%, and the vacancy rates above 5%. Finally, the Great Depression with high unemployment and low vacancy rates makes the Beveridge curve substantially flatter than it otherwise would have been. The Great Recession from 2007 to 2009 seems well aligned with the Beveridge curve even without the Great Depression.

2.1.3 Labor Productivity

Finally, we construct a historical series of labor productivity from January 1890 to December 2017, by dividing a series of nonfarm business real output by a series of private nonfarm employment.

We first obtain the following raw real output data: (i) Annual private nonfarm real gross domestic product, 1889–1957, from Kendrick (1961); (ii) annual nonfarm business real gross value added in billions of chained (2012) dollars, 1929–2017, from National Income and Product Accounts (NIPA) Table 1.3.6., line 3, at Bureau of Economic Analysis; (iii) quarterly nonfarm business real output index, from the first quarter of 1947 to the fourth quarter of 2017, from the BLS; (iv) the Miron-Romer (1990, Table 2) monthly industrial production index, January 1884–December 1940, not seasonally adjusted; and (v) the monthly industrial production index, January 1919–December 2017, seasonally adjusted, from Federal Reserve Bank of St. Louis.

We adjust the raw output data as follows. First, we seasonally adjust the Miron-Romer (1990) industrial production series with the X12 program from US Census Bureau, and quarterly splice the adjusted series to the Federal Reserve industrial production series in the first quarter of 1919. Second, we annually splice the Kendrick (1961) real output series to the NIPA series in the year 1929. Third, from January 1889 to December 1947, we use the Denton proportional first difference procedure to temporal disaggregate the annual nonfarm business real output series, with the monthly industrial production series as the indicator. Fourth, from January 1947 to December 2017, we use the Denton procedure to interpolate the BLS quarterly output series, with the industrial production series as the monthly indicator. Finally, we quarterly splice the pre-1947 monthly nonfarm business real output series to the post-1947 series in the first quarter of 1947.

We then obtain the following raw private nonfarm employment data: (i) Annual private nonfarm employment, number in thousands, 1890–1947, calculated as total civilian employment minus farm employment minus government employment, all from Weir (1992, Table D3); (ii) private nonfarm employment from CES, number in thousands, January 1939–December 2017, seasonally adjusted; (iii) index of factory employment, January 1889–December 1923, not seasonally adjusted, from NBER macrohistory series m08005; and (iv) total production worker employment in manufacturing, January 1919–March 1969, not seasonally adjusted, from NBER macrohistory series m08010b.

We adjust the raw private nonfarm employment data as follows. First, we seasonally adjust the NBER macrohistory series m08005 and m08010b with the X12 program, and quarterly splice the adjusted series m08005 to the adjusted series m08010b in the first quarter of 1919. Second, we use this monthly employment series as the indicator in the Denton proportional first difference procedure to temporally disaggregate Weir's annual series from 1890 to 1939. Finally, we quarterly splice the interpolated monthly private nonfarm employment series to the CES monthly series in the first quarter of 1939, yielding an uninterrupted series from January 1890 to December 2017.

We then divide the monthly nonfarm business real output series by the monthly private non-

farm employment series to obtain a labor productivity series from January 1890 to December 2017. From January 1947 to December 2017, we use the Denton procedure to benchmark the monthly labor productivity series to the quarterly nonfarm business real output per job series from the BLS. Benchmarking means that we impose the average of our monthly series within a given quarter to equal the same quarter's BLS observation. Finally, from January 1890 to December 1947, we quarterly splice in the first quarter of 1947 our pre-1947 series to the benchmarked post-1947 series.

Figure 4 plots the historical series of U.S. monthly nonfarm business real output, private nonfarm employment, and labor productivity (real output per person) from January 1890 to December 2017.

2.2 Labor Market Moments

We report labor market volatilities as well as higher moments for the unemployment rates.

2.2.1 Labor Market Volatilities

We study a standard set of second moments for the labor market for the long sample as well as for the postwar sample from January 1951 onward to facilitate comparison with prior studies (Shimer (2005). We take quarterly averages of the monthly unemployment rates, vacancy rates, and labor productivity series to convert to quarterly series. We then detrend the quarterly series in log deviations from the Hodrick-Prescott (HP, 1997) trend with a smoothing parameter of 1,600.

Table 1 shows that with the Great Depression in the sample, the volatility of civilian unemployment rates is 0.258, which more than doubles the volatility of 0.126 in the post-1951 sample. The unemployment-vacancy correlation is -0.79 based on the common sample from January 1919 onward but -0.92 in the postwar sample. As such, the Great Depression flattens somewhat the slope of the Beveridge curve (Figure 3). The vacancy volatility is 0.172 in the 1919–2017 sample, and is only slightly higher than 0.135 in the postwar sample. The standard deviation of the labor market tightness is 0.379 in the 1919–2017 sample, and is almost 50% higher than 0.256 in the post-1951 sample. As such, the historical sample has an important impact on this volatility estimate (Figure

2). More dramatically, the volatility of labor productivity is 0.012 in the postwar sample, but 0.039 in the 1890–2017 sample, which is more than three times the postwar volatility.

The volatility of private nonfarm unemployment rates is similar to that of civilian unemployment rates, 0.257 in the 1890–2017 sample, and 0.128 in the post-1951 sample (untabulated). The early 1920s only have a small impact on the volatility estimates. In the sample from January 1923 onward as in Zagorsky (1998), the vacancy rate volatility is 0.162, which is close to 0.172 in the full sample. The volatility of the labor market tightness is 0.357, which is also not far from 0.379 in the full sample. However, the volatility of civilian unemployment rates drops from 0.258 to 0.211, and the volatility of labor productivity from 0.039 to 0.025.

2.2.2 Unemployment Crises

To quantify the tail behavior in the U.S. unemployment rates in Figure 1, we follow Chatterjee and Corbae (2007) to fit a three-state Markov chain model via maximum likelihood. The aggregate state of the economy, $\xi_t \in \{g, b, c\}$, evolves through good (g), bad (b), and crisis (c) states with different employment prospects. Let the transition matrix of the Markov chain be given by:

$$P = \begin{bmatrix} p_{gg} & p_{bg} & p_{cg} \\ p_{gb} & p_{bb} & p_{cb} \\ p_{gc} & p_{bc} & p_{cc} \end{bmatrix}, \tag{1}$$

in which, for example, $p_{gb} \equiv \text{Prob}\{\xi_{t+1} = g | \xi_t = b\}$ is the probability of the economy being in state g next period conditional on the economy being in state b in the current period.

As in Chatterjee and Corbae (2007), the maximum likelihood estimate of p_{kj}, which is the (j,k)th element of the aggregate state transition matrix, is the ratio of the number of times the economy switches from state j to state k to the number of times the economy is in state j. Let, for example, $\mathbf{1}_{\{\xi_t = j\}}$ denote the indicator function that takes the value of one if the economy in period t is in state j and zero otherwise. The maximum likelihood estimate of p_{kj} is given by:

$$\hat{p}_{kj} = \frac{\sum_{t=1}^{T-1} \mathbf{1}_{\{\xi_{t+1}=k\}} \mathbf{1}_{\{\xi_t = j\}}}{\sum_{t=1}^{T-1} \mathbf{1}_{\{\xi_t = j\}}}. \tag{2}$$

In addition, the asymptotic standard error for $\hat{p}_{kj}$ is given by:

$$\text{Ste}(\hat{p}_{kj}) = \sqrt{\frac{\hat{p}_{kj}(1-\hat{p}_{kj})}{\sum_{t=1}^{T} \mathbf{1}_{\{\xi_t=j\}}}}. \tag{3}$$

In practice, we identify the good state, g, as months in which the unemployment rates are below the median. We define the crisis state, c, as months in which the unemployment rates are above or equal to 15%. The bad state, b, is then identified as months in which the unemployment rates are below 15% but above or equal to the median. The median is 5.54% for civilian unemployment rates, and 7.72% for private nonfarm unemployment rates. We choose the crisis cutoff of 15% judiciously such that it is relatively high, but there are still enough months in which the economy hits the crisis state to allow us to estimate the transition probabilities precisely.

Table 2 reports the estimated aggregate state transition matrix. The crisis state is persistent in that the probability of the economy remaining in the crisis state next period conditional on it being in the crisis state in the current period is 91.11% for civilian unemployment rates, and 95.36% private nonfarm unemployment rates. The estimates are also precise, with small standard errors of 4.25% and 1.71%, respectively. With probabilities of 8.89% and 4.64%, the economy switches from the crisis state to the bad state with the two unemployment rates series, respectively. Most important, unconditionally, the tail probability of the crisis state is estimated to be 2.93% for civilian unemployment rates, and 9.84% for private nonfarm unemployment rates.

3 The Model

Following Hall and Milgrom (2008), we construct a search model of equilibrium unemployment embedded with credible bargaining in determining the equilibrium wage.

3.1 The Setup

The model is populated by a representative household and a representative firm that uses labor as the single productive input. Following Merz (1995) and Andolfatto (1996), we use the representative

family construct, which implies perfect consumption insurance. The household has a continuum with a unit mass of members who are, at any point in time, either employed or unemployed. The fractions of employed and unemployed workers are representative of the population at large. The household pools the income of all the members together before choosing per capita consumption and asset holdings. Finally, the household is risk neutral with a time discount factor of β.

The representative firm posts a number of job vacancies, V_t, to attract unemployed workers, U_t. Vacancies are filled via a constant returns to scale matching function, $G(U_t, V_t)$, specified as:

$$G(U_t, V_t) = \frac{U_t V_t}{(U_t^\iota + V_t^\iota)^{1/\iota}}, \tag{4}$$

in which $\iota > 0$ is a constant parameter. This matching function, specified in Den Haan, Ramey, and Watson (2000), has the desirable property that matching probabilities fall between zero and one.

Define $\theta_t \equiv V_t/U_t$ as the vacancy-unemployment (V/U) ratio (labor market tightness). The probability for an unemployed worker to find a job per unit of time (the job finding rate), $f(\theta_t)$, is:

$$f(\theta_t) \equiv \frac{G(U_t, V_t)}{U_t} = \frac{1}{\left(1 + \theta_t^{-\iota}\right)^{1/\iota}}. \tag{5}$$

The probability for a vacancy to be filled per unit of time (the vacancy filling rate), $q(\theta_t)$, is:

$$q(\theta_t) \equiv \frac{G(U_t, V_t)}{V_t} = \frac{1}{(1 + \theta_t^\iota)^{1/\iota}}. \tag{6}$$

It follows that $q'(\theta_t) < 0$: An increase in the scarcity of unemployed workers relative to vacancies makes it harder to fill a vacancy. As such, θ_t is the market tightness from the firm's perspective.

The representative firm incurs costs in posting vacancies. Following Mortensen and Nagypàl (2007) and Pissarides (2009), we incorporate a fixed component in the unit cost per vacancy:

$$\kappa_t = \kappa_0 + \kappa_1 q(\theta_t), \tag{7}$$

in which κ_0 is the proportional cost, and κ_1 is the fixed cost. Both are nonnegative. The fixed cost

captures training, interviewing, and administrative setup costs of adding a worker to the payroll paid after a hired worker arrives but before wage bargaining takes place. The marginal cost of hiring from the proportional cost, $\kappa_0/q(\theta_t)$, is time-varying, but that from the fixed cost, κ_1, is constant.

Jobs are destroyed at a constant rate of $s > 0$ per period. Employment, N_t, evolves as:

$$N_{t+1} = (1 - s)N_t + q(\theta_t)V_t, \tag{8}$$

in which $q(\theta_t)V_t$ is the number of new hires. The size of the population is normalized to be unity, $U_t = 1 - N_t$. As such, N_t and U_t are also the rates of employment and unemployment, respectively.

The firm takes the labor productivity, X_t, as given. The law of motion for $x_t \equiv \log(X_t)$ is:

$$x_{t+1} = \rho x_t + \sigma \epsilon_{t+1}, \tag{9}$$

in which $\rho \in (0, 1)$ is the persistence, $\sigma > 0$ is the conditional volatility, and ϵ_{t+1} is an independently and identically distributed standard normal shock. The firm uses labor as the single input to produce output, Y_t, with a constant returns to scale production technology,

$$Y_t = X_t N_t. \tag{10}$$

The dividends to the firm's shareholders are given by:

$$D_t = X_t N_t - W_t N_t - \kappa_t V_t, \tag{11}$$

in which W_t is the equilibrium wage rate. Taking $q(\theta_t)$ and W_t as given, the firm posts an optimal number of job vacancies to maximize the cum-dividend market value of equity, denoted S_t:

$$S_t \equiv \max_{\{V_{t+\tau}, N_{t+\tau+1}\}_{\tau=0}^{\infty}} E_t \left[\sum_{\tau=0}^{\infty} \beta^{\tau} \left(X_{t+\tau} N_{t+\tau} - W_{t+\tau} N_{t+\tau} - \kappa_{t+\tau} V_{t+\tau} \right) \right], \tag{12}$$

subject to the employment accumulation equation (8) and a nonnegativity constraint on vacancies:

$$V_t \geq 0. \tag{13}$$

Because $q(\theta_t) > 0$, this constraint is equivalent to $q(\theta_t)V_t \geq 0$. As such, the only source of job destruction in the model is the exogenous separation of employed workers from the firm.[2]

Let λ_t denote the multiplier on the nonnegativity constraint $q(\theta_t)V_t \geq 0$. From the first-order conditions with respect to V_t and N_{t+1}, we obtain the intertemporal job creation condition:

$$\frac{\kappa_t}{q(\theta_t)} - \lambda_t = E_t \left[\beta \left(X_{t+1} - W_{t+1} + (1-s) \left(\frac{\kappa_{t+1}}{q(\theta_{t+1})} - \lambda_{t+1} \right) \right) \right]. \tag{14}$$

Intuitively, the marginal cost of hiring at time t equals the marginal value of employment to the firm, which in turn equals the marginal benefit of hiring at period $t+1$, discounted to t. The marginal benefit at $t+1$ includes the marginal product of labor, X_{t+1}, net of the wage rate, W_{t+1}, plus the marginal value of employment, which equals the marginal cost of hiring at $t+1$, net of separation. The optimal vacancy policy also satisfies the Kuhn-Tucker conditions:

$$q(\theta_t)V_t \geq 0, \quad \lambda_t \geq 0, \quad \text{and} \quad \lambda_t q(\theta_t)V_t = 0. \tag{15}$$

3.2 Credible Bargaining

To close the model, we need to specify how the wage rate, W_t, is determined in equilibrium. In the standard Diamond-Mortensen-Pissarides model, the wage rate is derived from the sharing rule per the outcome of a generalized Nash bargaining process between the employed workers and the firm. Let $0 < \eta < 1$ be the workers' relative bargaining weight and b the workers' value of unemployment activities. The Nash-bargained wage rate is:

$$W_t = \eta \left(X_t + \kappa_t \theta_t \right) + (1-\eta) b. \tag{16}$$

[2]This constraint does not bind in the model's simulations under the benchmark calibration. As such, the constraint does not affect our main quantitative results. However, because the constraint can be binding under at least some alternative parameterizations, we opt to impose the constraint in the solution algorithm for computational accuracy.

Although analytically simple, the baseline search model with the Nash wage requires a relatively high replacement ratio (the flow value of unemployment activities over the average marginal product of labor) to reproduce realistic labor market volatilities (Hagedorn and Manovskii 2008).

3.2.1 Institutional Background

We view the credible bargaining as a more appropriate modeling choice than the Nash bargaining for determining the equilibrium wage during the Great Depression. Cole and Ohanian (2004) show that after 1933 New Deal cartelization policies, which are designed to limit competition and increase labor bargaining power, increase wages and prices significantly and contribute greatly to the persistence of the Depression. In particular, real wages and relative prices in sectors covered by the cartelization policies rise after the National Industrial Recovery Act, and subsequently the National Labor Relations Act, are adopted, and remain high throughout the New Deal. In contrast, wages and prices in sectors not covered by these polices do not rise during this period.

Ohanian (2009) shows that prior to the New Deal, President Hoover's industrial labor program, along with the growing power of unions, contribute to real wage rigidity in the early stage of the Great Depression. In November 1929, Hoover met with the leaders of the major industrial firms, and requested them to not cut wages, to preferably even raise wages, and to spread work among employers. In return, labor union would not strike. By late 1931, real manufacturing average hourly earnings had raised more than 10%, and hours worked had declined more than 40%. In all, under Hoover's industrial labor program and Roosevelt's New Deal, the bargaining between firms and workers kept the wages insulated from the deteriorating labor market conditions even in the 1930s.

3.2.2 The Environment

Built on Binmore, Rubinstein, and Wolinsky (1986), Hall and Milgrom (2008) place a crucial distinction between a threat point and an outside option in the wage bargaining game. Bargaining takes time. Both parties make alternating offers which can be accepted, rejected to make a counteroffer, or rejected to abandon the bargaining altogether. In the Nash bargaining, disagreement leads imme-

diately to the abandonment of the bargaining game. As such, the relevant threat point is the outside options for both parties. In contrast, in the more realistic alternating bargaining, disagreement only leads to another round of alternating offers. The threat point is the payoff from another round of alternating offers, and outside options are taken only when abandoning the bargaining altogether.

The outside option for a worker is the flow value of unemployment. The outside option for the firm is to resume searching in the labor market, and its value is zero in equilibrium. During a period in which both parties engage in another round of alternating offers, the worker receives the flow value of unemployment, b, and the firm incurs the cost of delaying, $\chi > 0$, which can be interpreted as the cost of idle capital. During this period, the negotiation can break down with a probability of δ.

With this setup, the indifference condition for a worker when considering a wage offer, W_t, is:

$$J_{Nt}^{W} = \delta J_{Ut} + (1-\delta)\left(b + E_t[\beta J_{Nt+1}^{W'}]\right), \tag{17}$$

in which $J_t \equiv J(N_t, X_t)$ is the indirect utility function of the representative household. J_{Nt}^{W} is the marginal value of an employed worker to the household when accepting the wage offer from the employer. J_{Ut} is the marginal value of an unemployed worker to the household. Finally, $J_{Nt+1}^{W'}$ is the marginal value of an employed worker to the household when rejecting the firm's wage offer, W_t, in order to make a counteroffer of W'_{t+1} in the next period.

The indifference condition in equation (17) says that the payoff to the worker when accepting the wage offer from the firm, J_{Nt}^{W}, is just equal to the payoff from rejecting the offer. After rejecting the offer, with a probability of δ, the negotiation breaks down, and the worker returns to the labor market, leaving the household with the marginal value of an unemployed worker. With the probability of $1-\delta$, the worker receives the flow value of unemployment, b, for the current period, and makes a counteroffer of W'_{t+1} to the firm in the next period, with the payoff of $J_{Nt+1}^{W'}$.

The indifference condition for the firm when considering the worker's counteroffer, W'_t, is:

$$S_{Nt}^{W'} = \delta \times 0 + (1-\delta)\left(-\chi + E_t[\beta S_{Nt+1}^{W}]\right), \tag{18}$$

in which $S_{Nt}^{W'}$ is the marginal value of an employed worker to the firm when accepting the worker's counteroffer, and S_{Nt+1}^{W} is the marginal value of an employed worker to the firm when rejecting the worker's offer to make a counteroffer of W_{t+1} in the next period. Intuitively, equation (18) says that the firm is just indifferent between the payoff from accepting the worker's offer W_t' and the payoff from rejecting the offer to have an opportunity to make a counteroffer of W_{t+1} in the next period. When rejecting the offer, the firm pays the delaying cost of χ if the bargaining does not break down. When the negotiation does break down, the firm's payoff is zero.

The two indifference conditions in equations (17) and (18) collapse to those for the Nash bargaining when the probability of breakdown, δ, equals one. During the credible bargaining, it is optimal for each party to make a just acceptable offer. As in Hall and Milgrom (2008), we assume that the firm makes the first offer, which the worker accepts. As such, W_t is the equilibrium wage, and the delaying cost, χ, is never paid in equilibrium.

3.2.3 The Equilibrium Wage

The equilibrium wage, W_t, and the worker's counteroffer wage, W_{t+1}', can be further characterized. First, the marginal value of an unemployed worker to the household is:

$$J_{Ut} = b + \beta E_t \left[f(\theta_t) J_{Nt+1}^{W} + (1 - f(\theta_t)) J_{Ut+1} \right], \tag{19}$$

As such, the value of unemployment equals the flow value of unemployment, b, plus the discounted expected value in the next period. With a probability of $f(\theta_t)$, the unemployed worker lands a job, which delivers the value of J_{Nt+1}^{W}. Otherwise, the worker remains unemployed with a value of J_{Ut+1}.

In addition, the marginal value of an employed worker to the household is:

$$J_{Nt}^{W} = W_t + \beta E_t \left[(1 - s) J_{Nt+1}^{W} + s J_{Ut+1} \right]. \tag{20}$$

The equation says that the value of employment equals the flow value from the wage, W_t, plus the discounted expected value in the next period. With a probability of s, the employed worker

separates from the firm, and returns to the labor market as an unemployed worker with a value of J_{Ut+1}. Otherwise, the worker remains on the job, which delivers the value of J^W_{Nt+1}.

The wage offer issued by the firm to the worker, W_t, can be characterized as (Appendix B):

$$W_t = b + (1-\delta)\beta E_t\left[J^{W'}_{Nt+1} - J_{Ut+1}\right] - (1 - s - \delta f(\theta_t))\,\beta E_t\left[J^W_{Nt+1} - J_{Ut+1}\right]. \tag{21}$$

Intuitively, the wage offer from the firm increases in the flow value of unemployment, b. The second term in equation (21) says that if the bargaining does not breakdown, the wage offer also increases in the surplus that the worker would enjoy after making a counteroffer, W'_{t+1}, to the firm. From the last term in equation (21), the equilibrium wage also increases in the separation rate, s. As s goes up, the expected duration of the job shortens. As such, the worker requires a higher wage to remain indifferent between accepting and rejecting the wage offer. Finally, W_t increases in the job finding rate. As $f(\theta_t)$ rises, the worker's outside job market prospects improve, and the firm must offer a higher wage to make the worker indifferent. However, this impact of labor market conditions on W_t becomes negligible if the probability of breakdown in the bargaining, δ, goes to zero.

The wage offer of a worker to the firm, W'_t, can be expressed as:

$$W'_t = X_t + (1-\delta)\chi + \beta E_t\left[(1-s)S^{W'}_{Nt+1} - (1-\delta)S^W_{Nt+1}\right]. \tag{22}$$

Intuitively, W'_t increases in labor productivity, X_t, and the cost of delay to the firm, χ. A higher χ makes the firm more likely to accept a higher wage offer from the worker to avoid any delay. As W'_t contains a higher constant proportion because of a higher χ, W'_t becomes more insulated from labor market conditions. Because W'_t is the flow value of $J^{W'}_{Nt}$ from equation (20), $J^{W'}_{Nt}$ also becomes more insulated. More important, as $J^{W'}_{Nt}$ enters the second term in equation (21), the equilibrium wage, W_t, also becomes more insulated to aggregate conditions as a result of a higher χ.

From the last term in equation (22), an increase in the separation rate reduces the wage offer from the worker to the firm, W'_t. As s rises, the present value of profits produced by the worker

drops. To make the firm indifferent, the worker must reduce the wage offer. Also, the worker's offer, W_t', increases in the firm's surplus from accepting the offer, $S_{Nt+1}^{W'}$. In contrast, the worker's offer would be lower if the firm's surplus, S_{Nt+1}^{W}, from rejecting the offer to make a counteroffer, W_t, is higher. However, the quantitative impact of this channel would be negligible if the breakdown probability, δ, goes to one. As such, the worker's offer, W_t', increases with δ.

Finally, the two parties of the credible bargaining game would agree to accept the equilibrium wage, only if the joint surplus of the match is greater than the joint value of the outside options, J_{Ut}, as well as the joint present value of continuous delaying:

$$S_{Nt}^{W} + J_{Nt}^{W} > \max\left(J_{Ut}, E_t\left[\sum_{\tau=0}^{\infty}\beta^{\tau}(b-\chi)\right]\right) = J_{Ut}. \tag{23}$$

The last equality holds because the flow value of unemployment, b, is higher than $b-\chi$ (the delaying cost is positive). We verify that this condition holds in simulations.

3.3 Competitive Equilibrium

In equilibrium, the household receives the firm's dividends, and the goods market clears:

$$C_t + \kappa_t V_t = X_t N_t. \tag{24}$$

The competitive equilibrium consists of vacancy posting, $V_t \geq 0$, multiplier, $\lambda_t \geq 0$, consumption, C_t, and wages, W_t and W_t', such that: (i) V_t and λ_t satisfy the intertemporal job creation condition in equation (14) and the Kuhn-Tucker conditions (15); (ii) wages, W_t and W_t', satisfy the indifference conditions (17) and (18); and (iii) the goods market clears as in equation (24).

3.4 Computation

Because we focus on higher moments, we adopt the globally nonlinear projection algorithm in Petrosky-Nadeau and Zhang (2017). Because of risk neutrality and constant returns to scale, the state space consists of only log productivity, x_t. Employment, N_t, is not a state variable, although

the unemployment and vacancy rates do depend on N_t. In particular, we need to solve for the labor market tightness, $\theta_t = \theta(x_t)$, the multiplier function, $\lambda_t = \lambda(x_t)$, the equilibrium wage, $W_t = W(x_t)$, the worker's wage offer, $W'_t = W'(x_t)$, from the following five functional equations:

$$\frac{\kappa_t}{q(\theta_t)} - \lambda(x_t) = \beta E_t \left[\exp(x_{t+1}) - W(x_{t+1}) + (1-s) \left(\frac{\kappa_{t+1}}{q(\theta_{t+1})} - \lambda(x_{t+1}) \right) \right] \tag{25}$$

$$\begin{aligned} W(x_t) = {} & b + (1-\delta)\beta E_t \left[J_N^{W'}(x_{t+1}) - J_U(x_{t+1}) \right] \\ & - (1 - s - \delta f(\theta_t)) \beta E_t \left[J_N^{W}(x_{t+1}) - J_U(x_{t+1}) \right] \end{aligned} \tag{26}$$

$$J_U(x_t) = b + \beta E_t \left[f(\theta_t) J_N^W(x_{t+1}) + (1 - f(\theta_t)) J_U(x_{t+1}) \right] \tag{27}$$

$$J_N^W(x_t) = W(x_t) + \beta E_t \left[(1-s) J_N^W(x_{t+1}) + s J_U(x_{t+1}) \right] \tag{28}$$

$$J_N^{W'}(x_t) = W'(x_t) + \beta E_t \left[(1-s) J_N^{W'}(x_{t+1}) + s J_U(x_{t+1}) \right]. \tag{29}$$

In addition, $\theta(x_t)$ and $\lambda(x_t)$ must also satisfy the Kuhn-Tucker conditions (15).

We parameterize the conditional expectation in equation (25) as $\mathcal{E}_t \equiv \mathcal{E}(x_t)$, and four other functions, $W(x_t), J_U(x_t), J_N^W(x_t)$, and $J_N^{W'}(x_t)$. Following Christiano and Fisher (2000), we exploit a convenient mapping from $\mathcal{E}_t$ to policy and multiplier functions to eliminate the need to parameterize the multiplier function separately. After obtaining the parameterized $\mathcal{E}_t$, we first calculate $\tilde{q}(\theta_t) \equiv \kappa_t / \mathcal{E}_t$. If $\tilde{q}(\theta_t) < 1$, the nonnegativity constraint is not binding, we set $\lambda_t = 0$ and $q(\theta_t) = \tilde{q}(\theta_t)$. We then solve $\theta_t = q^{-1}(\tilde{q}(\theta_t))$, in which $q^{-1}(\cdot)$ is the inverse function of $q(\cdot)$ from equation (6). If $\tilde{q}(\theta_t) \geq 1$, the nonnegativity constraint is binding, we set $\theta_t = 0$, $q(\theta_t) = 1$, and $\lambda_t = \kappa_t - \mathcal{E}_t$.[3]

4 Quantitative Results

We calibrate the model in Section 4.1, and examine its key equilibrium properties in Section 4.2. We study the model's performance in explaining the higher moments of unemployment in Section 4.3 and the second moments of the labor market in Section 4.4. To shed light on the underlying

[3]We approximate the log productivity, x_t, with the discrete state space method of Rouwenhorst (1995). We use 17 grid points to cover the values of x_t, which are precisely within four unconditional standard deviations from the mean of zero. We use extensively the approximation toolkit in the Miranda and Fackler (2002) CompEcon Toolbox in Matlab. To obtain an initial guess, we use the loglinear solution to a simplified model without the fixed matching cost.

mechanisms, we conduct an extensive set of comparative statics in Section 4.5. Finally, in Section 4.6, we feed the log productivity in the data into the model, calculate its implied output, unemployment, and market tightness series, and to compare them with those the data.

4.1 Calibration

Following the bulk of the macro labor literature, our calibration strategy is to match the mean and the volatility of the postwar civilian unemployment rates. Because of the strong nonlinearity in the model, steady state relations hold poorly in simulations, and we do not use these relations.

Table 3 lists the parameter values for the monthly benchmark calibration of the model. Following Gertler and Trigari (2009), we set the time discount factor, β, to be $0.99^{1/3}$ and the persistence of the log labor productivity, ρ, to $0.95^{1/3}$. We then calibrate its conditional volatility, σ, to be 0.00635 to match the standard deviation of 0.012 for the labor productivity in the postwar data (Table 1). We set the separation rate, s, to be 3.5%, which is the average total nonfarm separation rate from December 2000 to December 2017 in JOLTS. For the elasticity parameter in the matching function, ι, we set it to be 1.25, which is close to that in Den Haan, Ramey, and Watson (2000).

Following Hall and Milgrom (2008), we calibrate the flow value of unemployment to be 0.71. The probability of breakdown in bargaining, δ, is 0.1, which is close to the value of 0.0055 in their daily calibration (with 20 working days per month). The delaying cost parameter, χ, is set to be 0.25, which is close to their value of 0.27. Finally, to calibrate the recruiting cost parameters, κ_0 and κ_1, we target the first and the second moments of civilian unemployment rates in the postwar sample. The average unemployment rate in this sample is 5.83%, and the unemployment volatility is 0.126 (Table 1). We end up with the recruiting cost parameters, $\kappa_0 = 0.2$ and $\kappa_1 = 0.35$, which imply a mean of 5.81% and a volatility of 0.126 for the unemployment rate in normal periods.

4.2 Properties of the Competitive Equilibrium

Before presenting quantitative results, we study the model's theoretical properties in equilibrium.

4.2.1 Key Variables

Using the model's competitive equilibrium, Figure 5 plots several key variables against the log labor productivity, x_t. The variables all exhibit sensible cyclical properties.

Specifically, the marginal value of employment to the firm, which is the conditional expectation in equation (25), $\mathcal{E}_t$, is procyclical. The labor market tightness, θ_t, and the job finding rate of unemployed workers, $f(\theta_t)$, are also both procyclical. In contrast, the vacancy filling rate, $q(\theta_t)$, is countercyclical. Finally, both the equilibrium wage, W_t, which is the wage offered by the firm to the worker, as well as the wage offered by the worker to the firm, W_t', are both procyclical.

4.2.2 Stationary Distribution

We simulate the model economy for one million monthly periods from its stationary distribution. To reach the stationary distribution, we start at the initial condition of zero for the log labor productivity, and simulate the economy for 6,000 months. Panel A of Figure 6 presents the scatter plot of the unemployment rate against the log productivity in simulations. The relation is strongly nonlinear. When the log productivity is above its mean of zero, unemployment goes down only slightly. However, when the log productivity is below its mean, unemployment goes up drastically. The correlation between unemployment and log productivity is -0.82. Panel B plots the vacancy rate, θ_t, against the log productivity. Although the relation is nonlinear, the nonlinearity is not nearly as strong as that of unemployment in Panel A. The V_t-x_t correlation is near perfect at 0.96.

Panels C and D report the empirical cumulative distribution functions of the unemployment and vacancy rates. Unemployment is highly skewed. Its 2.5 percentile, 4.03%, is close to the median, 5.61%, but the 97.5 percentile is far away, 17.37%. The 99 percentile is 21.36%, and the maximum rate is almost 50%. In contrast, the empirical distribution of the vacancy rates is close to symmetric. Its 2.5, 50, and 97.5 percentiles are 2.62%, 6.06%, and 12.11%, respectively.

4.2.3 Nonlinear Impulse Responses

We also calculate nonlinear impulse response functions. To show their state dependence, we do so from three different starting points: bad, median, and good economies. The bad economy is the 5 percentile of the model's bivariate stationary distribution of employment and log productivity, the median is the median, and the good economy is the 95 percentile. As noted, although employment is not a state variable, unemployment and vacancy rates depend on employment in the model. Across the bad, median, and good economies, the unemployment rates are 14.36%, 5.61%, and 4.13%, and the log labor productivity levels are $-0.0567, 0$, and 0.0567, respectively. Both positive and negative one-standard-deviation shocks to the log productivity are examined.

Panels A to C of Figure 7 report responses in the labor market tightness. We observe that the responses are substantially larger in the bad economy than in the good economy. In the bad economy, a positive one-standard-deviation shock to the log productivity increases the tightness by 25.43%. In contrast, the response is only 7.42% in the good economy, and is less than 30% of the response in the bad economy. A negative impulse decreases the tightness by 7.32% in the good economy, which is slightly more than 30% of the response in the bad economy, 23%.

We also see large and asymmetric responses in unemployment. After a negative impulse, the unemployment rate shoots up 1.44% in the bad economy (Panel D). This response is about 11.7 times as large as that of 0.12% in the good economy (Panel F). From Panel E, the response in the median economy is only 0.4%, which is much closer to that in the good economy than to the bad economy.

Panels G to I show limited wage responses. Even starting from the bad economy, a negative one-standard-deviation impulse reduces the equilibrium wage only by 0.66%, which is merely 2.85% of the response in the market tightness, 23%. A positive impulse raises the wage only by 0.66%, which is about 2.6% of the response in the market tightness, 25.43%. Clearly, consistent with Hall and Milgrom (2008), the equilibrium wage in the credible bargaining model is insulated from labor market conditions. More important, this insulation holds up quantitatively even in the bad

economy, and forces negative shocks to be absorbed mostly by unemployment, giving rise to crises.

4.3 Explaining Higher Moments of Unemployment

Most important, can the model explain quantitatively the unemployment crisis dynamics in the data, including the aggregate state transition matrix and the tail probability of the crisis state in Table 2? To this end, from the model's stationary distribution, we repeatedly simulate 25,000 artificial samples, each of which contains 1,536 monthly periods. The sample length matches the number of months in the data from January 1890 to December 2017.

Because crises do not occur in every simulated sample, we split the 25,000 samples into two groups, non-crisis and crisis samples. If the maximum unemployment rate in an artificial sample is greater than or equal to 15%, we categorize it as a crisis sample (otherwise a non-crisis sample). The cutoff threshold of 15% is consistent with our empirical treatment of the historical data (Table 2). On each crisis sample (i.e., conditional on at least one crisis), we calculate the state transition matrix and unconditional probabilities of the states using the exactly same procedure as in Table 2. We then report the cross-simulation averages and standard deviations across the crisis samples.

Table 4 reports the model output. A comparison with Table 2 shows that the model seems to do a good job in explaining the large unemployment dynamics in the data. The probability of the economy remaining in the crisis state next period conditional on the crisis state in the current period is 91.8%, which is close to 91.1% for civilian unemployment rates in the data, but somewhat lower than 95.4% for private nonfarm unemployment rates. In addition, the unconditional probability of the crisis state in the model is 4.77%, which is also close to 2.93% in the data for civilian unemployment rates, but lower than 9.84% for private nonfarm unemployment rates. The cross-simulation standard deviation of the 4.77% estimate in the model is 4.31%. This level of dispersion is perhaps not surprising for a tail probability estimate. In all, the model's estimate seems empirically plausible.

The skewness of the model's unemployment rates is 2.06, and the kurtosis 7.9, with cross-simulation standard deviations of 0.59 and 3.62, respectively (untabulated). The skewness in the

model is close to 2.29 for civilian unemployment rates and 2.15 for private nonfarm unemployment rates in the historical series, but the kurtosis is lower than 11.12 and 9.61 in the data, respectively.

4.4 Explaining Labor Market Volatilities

The crisis dynamics in the model have important implications for the second moments such as volatilities and correlations, which are the traditional focus in the macro labor literature. In particular, it can be misleading to focus only on the second moments in normal periods (non-crisis samples). The second moments in the crisis samples can deviate from those in normal periods.

Panel A of Table 5 reports the results conditional on the non-crisis samples. The unemployment volatility is 0.126, which matches that in the postwar data (see Table 1). Although not a direct target, the standard deviation of labor market tightness is 0.27 in the model, which is close to 0.256 in the data. However, the model predicts a vacancy volatility of 0.168, which overshoots 0.135 in the data. Although negative, the unemployment-vacancy correlation is -0.68 in the model, which is lower in magnitude than -0.92 in the data. Overall, consistent with Hall and Milgram (2008), the credible bargaining model explains the unemployment volatility puzzle.

However, focusing only on normal periods suffers from a selection bias that arises from ignoring the crisis samples. Panel B reports the results conditional on the crisis samples. The unemployment volatility rises to 0.156. However, this estimate falls short of 0.258 in the 1890–2017 sample in the data (Table 1), as we calibrate the model's volatility of the labor productivity only to the postwar sample. The volatilities of vacancy and labor market tightness increase somewhat to 0.18 and 0.3, respectively. The 0.18 estimate is close to 0.17, but the 0.3 estimate is lower than 0.38 in the historical sample. The model also predicts that the unemployment-vacancy correlation drops somewhat from -0.68 in the non-crisis samples to -0.6 in the crisis samples. This result is consistent with a flatter Beveridge curve in the historical sample than in the postwar sample (Figure 3). However, the magnitude of these correlations in the model is lower than those in the data.

The quantitative results are intrinsically linked to the nonlinear dynamics in Figures 6. Pre-

cisely because unemployment exhibits a long right tail, ignoring crises by focusing only on the second moments in normal periods understates its volatility. However, because the nonlinearity of the vacancy rate is weaker than that of unemployment, ignoring crises does not materially affect its volatility, but does overstate the unemployment-vacancy correlation.

4.5 Comparative Statics

To shed light on the economic mechanisms behind our quantitative results, we conduct an array of comparative statics: (i) the probability of breakdown in bargaining $\delta = 0.15$; (ii) the delaying cost $\chi = 0.20$; (iii) the proportional cost of vacancy posting $\kappa_0 = 0.15$; (iv) the fixed cost of vacancy posting $\kappa_1 = 0.3$; (v) the separation rate $s = 0.04$; and (vi) the curvature parameter of the matching function $\iota = 0.9$. In each experiment, all the other parameters remain identical to the benchmark calibration. We quantify how the results in Tables 4 and 5 change as we vary each parameter.

Table 6 reports the results for the crisis moments, and Table 7 for the second moments of the labor market in non-crisis samples (we omit the second moments in crisis samples to save space). From Panel A of Table 6, increasing the probability of breakdown in negotiation, δ, weakens the crisis dynamics. The persistence of crisis weakens from 0.918 to 0.823, and the unconditional crisis probability falls from 4.77% to 1.76%. Panel A of Table 7 shows that raising δ decreases the labor market volatilities. Intuitively, a higher probability of breakdown in negotiation brings credible bargaining closer to the Nash bargaining, in which $\delta = 1$, giving rise to more flexible wages. As such, a higher δ makes the equilibrium wage less insulated to labor market conditions. In bad times, as the productivity drops, the wage also falls, providing the firm with more incentives to creating jobs. As such, the unemployment volatility falls, and the crisis dynamics weaken.

The delaying cost is also important for explaining the crisis moments. From Panel B of Table 6, reducing χ from 0.25 under the benchmark calibration to 0.2 lowers the persistence of the crisis state from 0.918 to 0.784, and the unconditional crisis probability from 4.77% to 1.31%. Panel B of Table 7 shows further that reducing χ lowers the unemployment volatility from 0.126 to 0.068 in normal

periods. Intuitively, a lower delaying cost makes the equilibrium wage more responsive to labor market conditions. As such, labor market volatilities are lowered, and the crisis dynamics dampened.

The proportional and the fixed costs of vacancy posting impact the results in the same direction as the cost of delaying, but to a lesser extent quantitatively. From Table 6, reducing κ_0 to 0.15 lowers the persistence of the crisis state slightly to 0.886 and the unconditional probability to 3.79%. Similarly, reducing κ_1 to 0.3 drops the persistence of the crisis state slightly to 0.891 and the unconditional probability to 3.94%. From Table 7, reducing κ_0 and κ_1 also lowers the unemployment volatility somewhat to 0.119 and 0.114, respectively. Intuitively, reducing vacancy costs stimulates job creation flows to starve off unemployment crises. In particular, the fixed cost gives rise to the downward rigidity in the marginal cost of hiring. Reducing the fixed cost weakens the rigidity, allowing the marginal cost of hiring to decline and more jobs to be created in recessions.

From Panel E of Table 6, raising the separation rate, s, to 4% makes the crises more frequent and persistent. The persistence goes from 0.918 to 0.938, and the unconditional probability from 4.77% to 9.97%. Intuitively, because jobs are destroyed at a higher rate, all else equal, the economy is more capable of offsetting job destruction flows through job creation. As such, the crisis dynamics are strengthened. However, from Table 7, a higher s reduces the labor market volatilities slightly.

From Panel F of Table 6, reducing the curvature of the matching function, ι, from 1.25 to 0.9 strengthens the crisis dynamics. The persistence of the crisis state increases to 0.944, and its unconditional probability to 5.78%. Intuitively, a decrease in ι increases the elasticity of new hires with respect to vacancies. (This elasticity is given by $1/(1+\theta_t^{\iota})$, and a lower ι means a higher elasticity for $\theta > 1$, which holds most of the time in the model's simulations.) As vacancies fall in recessions, new hires drop faster with a lower ι, meaning that the congestion effect for unemployed workers becomes more severe. As such, the crisis dynamics are reinforced. However, a lower ι reduce the unemployment volatility to 0.108 (Panel F in Table 7).

4.6 Accounting for the Great Depression

Finally, going beyond matching moments, we perform a more stringent test of the model by feeding the log labor productivity in the Great Depression into the model. We calculate the implied output, unemployment, and market tightness in the model, and compare them with those in the data.

We start with the labor productivity in the data (Figure 4). Taking the log yields the monthly log productivity, which we detrend via the Hamilton (2018) method by regressing the 12-month-ahead values on the values of the most recent 12 months as of the current month, with a constant. The cyclical component of the log productivity is the residual series from the regression.[4] Panel A of Figure 8 plots the cyclical component of the log productivity from January 1929 to December 1939. The large drop in 1933 is clearly visible, with the bottom of the log productivity close to -0.3.

The model does a good job in tracing out the output drop in the data (Panel B). The predicted output tracks the cyclical component of output in the data, with a high correlation of 0.58. (We again detrend the log real output via the Hamilton method.) The model predicts that output drops by over 40% relative to its long run average in 1933. The magnitude of the drop is somewhat larger than about 30% in the data. More important, the model shows some potential in explaining the unemployment crisis in the Great Depression (Panel C). For example, the model predicts that in 1933 the unemployment rate reaches over 35%, which is higher than the maximum civilian unemployment rate of 25.5%, but close to the maximum private nonfarm unemployment rate of 35.5%.

More seriously, Panel C reveals a lack of persistence of high unemployment rates in the model than in the data in the Great Depression. During the 1929–1939 decade, the unemployment rates in the data are persistently high. Civilian unemployment rates are on average 13.16%, and private nonfarm unemployment rates 18.85%. In contrast, despite a few upward spikes, the unemployment rates in the model are often normal, especially between 1934 to 1937. The lack of persistence in

[4]We have experimented with the HP filter with a smoothing parameter of 129,600 per Ravn and Uhlig (2002) for the monthly series, but found the results to be excessively sensitive to the chosen smoothing parameter. Because our accounting exercise requires the model to match every sample observation in the Great Depression, not just a few key moments, we opt to use the more robust Hamilton (2018) method to detrend the monthly series of the log productivty.

high unemployment rates also shows up in the labor market tightness. While the market tightness in the data is persistently low in the 1930s, the market tightness in the model fluctuates greatly after 1934 and fails to match this aspect of the data.

5 Conclusion

A search model of equilibrium unemployment, when calibrated to the mean and volatility of unemployment rates in the postwar sample, can potentially explain the unemployment crisis in the Great Depression. The key ingredient of the model is the Hall and Milgrom (2008) credible bargaining game for determining the equilibrium wage. The limited responses of the wages to conditions in the labor market, along with the congestion externality from matching frictions, cause the unemployment rate to rise sharply in recessions but to decline gradually in booms. The frequency and severity of the unemployment crises in the model are quantitatively consistent with the U.S. historical series. However, when we feed the measure labor productivity in the data into the model, the predicted unemployment crisis is less persistent than that in the 1930s.

A Data

We describe our detailed procedures to construct the historical samples for unemployment rates in Appendix A.1, vacancy rates in Appendix A.2, and labor productivity in Appendix A.3.

A.1 Unemployment Rates

We construct the historical series for civilian unemployment rates in Appendix A.1.1 and for private nonfarm unemployment rates in Appendix A.1.2, both from January 1890 to December 2017.

A.1.1 Civilian Unemployment Rates

From January 1948 to December 2017, we use the seasonally adjusted civilian unemployment rate series from Bureau of Labor Statistics at US Department of Labor. No adjustment is necessary.

From January 1930 to December 1947, we use the Denton (1971) proportional first difference procedure to interpolate Weir's (1992) annual series of civilian unemployment rates. We use the proportional first difference variant of the "denton_uni" routine in Matlab provided by Quilis (2013). The monthly indicator series in the interpolation is constructed from the monthly unemployment rates from NBER macrohistory files (chapter 8: Income and employment, http://www.nber.org/databases/macrohistory/contents/chapter08.html). We impose the monthly average of the interpolated series in a given year to equal the year's annual value in Weir.

We construct the monthly indicator series from January 1930 to December 1947 as follows:

- From January 1930 to February 1940, we use as the monthly indicator values the seasonally adjusted unemployment rates from NBER macrohistory series m08292a (April 1929–June 1942. Source: National Industrial Conference Board, published by G. H. Moore Business Cycle Indicators, vol. II, p. 35 and p. 123).

- From March 1940 to December 1946, we use as the monthly indicator values the seasonally adjusted unemployment rates from NBER macrohistory series m08292b (March 1940–December 1946. Source: US Bureau of the Census, Current Population Reports, Labor Force series P-50, no. 2, 13, and 19).

- From January 1947 to December 1947, we construct the monthly indicator values as follows. We first obtain the monthly unemployment rates (not seasonally adjusted) from January 1947 to December 1966 from NBER macrohistory series m08292c. (Source: Employment and Earnings and Monthly Report on the Labor Force, vol. 13, no. 9, March 1967). We pass the entire 1947–1966 series through the X-12-ARIMA seasonal adjustment program from US Census Bureau. We then take the seasonally adjusted series from January 1947 to December of 1947.

From January 1890 to December 1929, we use the Denton procedure interpolate Weir's (1992) annual civilian unemployment rates with the credit spread series from NBER macrohistory files

as the monthly indicator. (Monthly unemployment rates are not available prior to April 1929 in NBER macrohistory files.) We again require the monthly average of the interpolated series in a given year to equal the year's annual value in Weir.

We construct the monthly indicator series from January 1890 to December 1929 as follows:

- We obtain American railroad bond yields, high grade, from NBER macrohistory series m13019 (January 1857–January 1937. Source: Frederick R. Macaulay, 1938, Appendix Table 10, p. A142–A161). We also obtain US railroad bond yields index from NBER macrohistory series m13019a (January 1857–December 1934, Source: Frederick R. Macaulay, 1938, Appendix Table 10, column 4, p. A142–A161). Subtracting series m13019 from m13019a yields the railroad credit spread series from January 1857 to December 1934.

- We obtain Moody's seasoned Aaa and Baa corporate bond yields, monthly, from Federal Reserve Bank of St. Louis. The sample is from January 1919 to June 2018. Subtracting the Aaa yields from the Baa yields, we obtain the credit spread series over the same sample period.

- We quarterly splice the railroad credit spread series to the Moody's credit spread series in the first quarter of 1919. Quarterly splicing means that we rescale the railroad series so that its average in the first quarter of 1919 equals the average of the Moody's series in the same quarter. Doing so yields an uninterrupted credit spread series from January 1857 to June 2018. We take the values from January 1890 to December 1929 as the monthly indicator.

A.1.2 Private Nonfarm Unemployment Rates

From January 1890 to December 1947, we use the Denton (1971) proportional first difference procedure to interpolate Weir's (1992, Table D3, last column) annual series of private nonfarm unemployment rates. The monthly indicator from January 1890 to December 1929 is the spliced credit spread series constructed in Appendix A.1.1. From January 1930 onward, the monthly indicator is the monthly unemployment rate series obtained from NBER macrohistory files (Appendix A.1.1). The monthly average of the interpolated series in a given year is set to that year's annual value in Weir.

From January 1948 to December 2017, we follow Weir (1992) to calculate private nonfarm unemployment rates as (Civilian labor force − Civilian employment)/(Civilian labor force − (Farm employment + Government employment)). In the numerator, both terms should subtract the sum of farm and government employment to yield private nonfarm labor force and private nonfarm employment, respectively. As such, the two subtractions cancel, and the numerator is simply civilian unemployment, which we measure as series LNS13000000 from the Current Population Survey (CPS, January 1948–December 2017, seasonally adjusted). We measure civilian labor force as the CPS series LNS11000000 (January 1948–December 2017, seasonally adjusted).

We back out the sum of farm and government employment as the CPS civilian employment (series LNS12000000, January 1948–December 2017, seasonally adjusted) minus private nonfarm

employment from the Current Employment Statistics (CES) survey (series CES0500000001, January 1939–December 2017, seasonally adjusted). While CPS and CES have important differences (Bowler and Morisi 2006), Weir also uses CES-based government employment data. In all, we measure private nonfarm unemployment rates as: Civilian unemployment/(Civilian labor force − (Civilian employment from CPS − Private nonfarm employment from CES)).

A.2 Vacancy Rates

We construct a historical series for the vacancy rates from January 1919 to December 2017.

A.2.1 Vacancy Series

From December 2000 to December 2017, we obtain the seasonally adjusted job openings (series JTS00000000JOL, total nonfarm, level in thousands) from the Job Openings and Labor Turnover Survey (JOLTS) released by US Bureau of Labor Statistics. This series contains government job openings. Because the series for government job openings are not available prior to December 2000 when JOLTS becomes available, we use total nonfarm job openings (instead of total private nonfarm job openings, series JTS10000000JOL) throughout the long historical sample to be consistent.

From January 1995 to November 2000, we use the seasonally adjusted composite print and online help-wanted index from Barnichon (2010). The Barnichon series, ranging from January 1995 to December 2014, is from Regis Barnichon's Web site. We quarterly splice the Barnichon series to the JOLTS series in the first quarter of 2001. Quarterly splicing means that we rescale the Barnichon series so that its monthly average in the first quarter of 2001 equals the monthly average of the JOLTS series in the same quarter.

From January 1951 to December 1994, we use the seasonally adjusted help-wanted advertising index from the Conference Board. The Conference Board series goes from January 1951 to June 2010. We quarterly splice the Conference Board series to the (spliced) Barnichon series in the first quarter of 1995. Quarterly splicing means that we rescale the Conference Board series so that its monthly average in the first quarter of 1995 equals the monthly average of the Barnichon series (already spliced to the JOLTS series per the last paragraph) in the same quarter. We switch to the Barnichon series in January 1995 because advertising for jobs over the internet has become more and more prevalent since the mid-1990s, making the print help-wanted index from the Conference Board increasingly unrepresentative. A comparison between between the Barnichon series and the Conference Board series shows that the two series have diverged significantly since 1996.

From January 1919 to December 1950, we use the Metropolitan Life Insurance company (MetLife) help-wanted advertising index. The MetLife series is from the NBER macrohistory files (series m08082a, January 1919–August 1960, not seasonally adjusted). To seasonally adjust the series, we pass the entire series through the X-12-ARIMA program from US Census Bureau. We then quarterly splice the seasonally adjusted MetLife series to the (spliced) Conference Board series

in the first quarter of 1951. Quarterly splicing means that we rescale the MetLife series so that its monthly average in the first quarter of 1951 equals the monthly average of the Conference Board series (already spliced to the rescaled Barnichon series per the last paragraph) in the same quarter.

A.2.2 Labor Force Series

To convert the vacancy series into a series of vacancy rates, we need a series of the labor force. From January 1948 to December 2017, we obtain the monthly civilian labor force over 16 years of age from the Current Population Survey released by US Bureau of Labor Statistics (series LNS11000000, seasonally adjusted, number in thousands). No additional adjustment is necessary.

From January 1890 to December 1947, we use Weir's (1992) annual series of civilian labor force (1890–1990, 14 years and older through 1946, 16 and older afterward, number in thousands). We use the Denton proportional first difference procedure to interpolate Weir's annual series to monthly, using a vector of ones as the indicator. Because the labor force is a stock variable, we require the first monthly observation of a given year to equal that year's observation in Weir. We then annually splice the interpolated Weir series to the CPS series in the year of 1948. Annual splicing means that we rescale the interpolated Weir series so that its monthly average in 1948 equals the monthly average of the CPS series in the same year.

A.2.3 Vacancy Rates Series

Dividing the vacancy series constructed in Appendix A.2.1 by the labor force series in Appendix A.2.2 yields a long historical series of vacancy rates from January 1919 to December 2017.

A.3 Labor Productivity

To construct a historical series of labor productivity from January 1890 to December 2017, the basic idea is to calculate the ratio of private nonfarm real output over private nonfarm employment.

A.3.1 Nonfarm Business Real Output

We obtain the following raw real output data:

- Private nonfarm real gross domestic product, 1889–1957, annual, Kendrick (1961, Table A-XXIII, p. 338–340, http://www.nber.org/chapters/c2246.pdf).
- Nonfarm business real gross value added in billions of chained (2012) dollars, Table 1.3.6., line 3, annual, 1929–2017, National Income and Product Accounts (NIPA), Bureau of Economic Analysis.
- Nonfarm business real output index, quarterly, from the first quarter of 1947 to the fourth quarter of 2017, from Bureau of Labor Statistics (BLS, series PRS85006043).

- The Miron-Romer (1990, Table 2, p. 336–337) monthly index of industrial production, January 1884–December 1940, not seasonally adjusted. We set the missing value in March 1902 the average of the values in February and April of the same year. For seasonal adjustment, we pass the entire series through the X-12-ARIMA program from US Census Bureau.
- Industrial production index from Federal Reserve Bank of St. Louis (series INDPRO), monthly, January 1919–December 2017. Seasonally adjusted.

We adopt the following procedure to adjust the raw output data:

- We quarterly splice the seasonally adjusted Miron-Romer industrial production series to the Federal Reserve series in the first quarter of 1919. Quarterly splicing means that we rescale the Miron-Romer series so that its monthly average in the first quarter of 1919 equals the monthly average of the Federal Reserve series in the same quarter. Splicing gives us an interrupted series of industrial production from January 1884 to December 2017.
- We annually splice the Kendrick's (1961) nonfarm business real output series from 1889 to 1929 to the NIPA nonfarm business real output series from 1929 to 1947 in the year 1929. We rescale the Kendrick series so that its value in 1929 equals the value for the NIPA series in the same year. Splicing gives us an uninterrupted annual real output series from 1889 to 1947.
- From January 1889 to December 1947, we use the Denton proportional first difference procedure to interpolate the annual nonfarm business real output, with the monthly industrial production series as the indicators.
- From January 1947 to December 2017, we use the Denton proportional first difference procedure to interpolate the BLS quarterly series of nonfarm business real output, with the monthly industrial production series as the indicators.
- Finally, we quarterly splice the above two monthly series of nonfarm business real output in the first quarter of 1947. We rescale the pre-1947 series so that its monthly average in the first quarter of 1947 equals the monthly average of the post-1947 series in the same quarter.

A.3.2 Private Nonfarm Employment

We obtain the following raw private nonfarm employment data:

- Private nonfarm employment from Weir (1992, Table D3, annual series, 1890–1947). We calculate private nonfarm employment as total civilian employment minus farm employment minus government employment, all of which are from Weir's Table D3.
- Private nonfarm employment from Current Employment Statistics released by BLS (series CES0500000001, number in thousands, seasonally adjusted, monthly series, January 1939–December 2017).

- Index of factory employment, NBER macrohistory series m08005, monthly, January 1889–December 1923. Not seasonally adjusted. Source: H. Jerome, Migration and Business Cycles, NBER Publication 9, p. 248. For seasonal adjustment, we pass the entire series through the X-12-ARIMA program from US Census Bureau.

- Total production worker employment in manufacturing, NBER macrohistory series m08010b, monthly, number in thousands, January 1919–March 1969. Not seasonally adjusted. Source: BLS Bulletin, Employment and Earnings Statistics for the Unites States, 1909–1960 (for 1919–1958), and 1909–1966 (for 1959–1967); Employment and Earnings (for September 1967–March 1969). For seasonal adjustment, we pass the entire series through the X-12-ARIMA program.

We adopt the following procedure to adjust the raw employment data:

- We quarterly splice NBER macrohistory series m08005 to NBER macrohistory series m08010b, both seasonally adjusted, in the first quarter of 1919. In particular, we rescale the seasonally adjusted series m08005 so that its monthly average in the first quarter of 1919 equals the monthly average of the seasonally adjusted series m08010b in the same quarter. Doing so yields an uninterrupted monthly employment series from January 1889 to December 1939.

- We use this monthly employment series as the indicator in the Denton proportional first difference procedure to interpolate Weir's annual series from 1890 to 1939. Because private nonfarm employment is a stock variable, we require the first monthly observation of a given year to equal that year's observation in Weir. Doing so yields a monthly private nonfarm employment series from January 1890 to December 1939.

- We quarterly splice this monthly private nonfarm employment series to the CES monthly series around the first quarter of 1939. We rescale the interpolated Weir series so that its monthly average in the first quarter of 1939 equals the monthly average of the CES series in the same quarter. Doing so yields a monthly series from January 1890 to December 2017.

A.3.3 Private Nonfarm Labor Productivity

We first obtain the nonfarm business real output per job from BLS (series PRS85006163, quarterly, 1947Q1–2017Q4, index, base year = 2012).

We then divide the monthly nonfarm business real output series constructed in Appendix A.3.1 by the monthly private nonfarm employment series constructed in Appendix A.3.2 to obtain a monthly labor productivity series from January 1890 to December 2017.

From January 1947 to December 2017, we use the Denton proportional first difference procedure to benchmark our monthly labor productivity series to the BLS quarterly labor productivity series. Benchmarking means that we impose the average of our monthly series within a given quarter to equal that quarter's BLS observation. Alas, the standard Denton procedure induces a transient,

artificial movement at the beginning of the series (Dagum and Cholette 2006, Chapter 6). We remove this transient movement with the Cholette (1984) modification.

Finally, from January 1890–December 1947, we quarterly splice (in the first quarter of 1947) our monthly labor productivity series to the benchmarked monthly series from 1947 onward. In particular, we scale the pre-1947 series so that its monthly average in the first quarter of 1947 equals the monthly average of the post-1947 series.

B Derivations

To prove equation (21), we plug equations (19) and (20) into equation (17) to obtain:

$$W_t+\beta E_t\left[(1-s)J^W_{Nt+1}+sJ_{Ut+1}\right]=b+\delta\beta E_t\left[f(\theta_t)J^W_{Nt+1}+(1-f(\theta_t))J_{Ut+1}\right]+(1-\delta)\beta E_t\left[J^{W'}_{Nt+1}\right]. \tag{B.1}$$

Solving for W_t yields:

$$W_t=b+[\delta f(\theta_t)-(1-s)]\beta E_t\left[J^W_{Nt+1}\right]+[\delta(1-f(\theta_t))-s]\beta E_t\left[J_{Ut+1}\right]+(1-\delta)\beta E_t\left[J^{W'}_{Nt+1}\right]. \tag{B.2}$$

Rearranging the right-hand side yields equation (21).

To characterize the worker's counteroffer, W'_t, as in equation (22), we first rewrite equation (12) recursively (while making explicitly the dependence of S_t on W_t with the notation S^W_t):

$$S^W_t=X_tN_t-W_tN_t-\kappa_tV_t+\lambda_tq(\theta_t)V_t+\beta E_t\left[S^W_{t+1}\right], \tag{B.3}$$

The first-order condition with respect to V_t yields:

$$\frac{\kappa_0}{q(\theta_t)}+\kappa_1-\lambda_t=\beta E_t\left[S^W_{Nt+1}\right]. \tag{B.4}$$

Also, replacing W_t with W'_t in equation (B.3) and differentiating with respect to N_t yield:

$$S^{W'}_{Nt}=X_t-W'_t+(1-s)\beta E_t\left[S^{W'}_{Nt+1}\right]. \tag{B.5}$$

Plugging equation (B.4) into the firm's indifference condition (18) yields:

$$S^{W'}_{Nt}=(1-\delta)\left[\frac{\kappa_0}{q(\theta_t)}+\kappa_1-\lambda_t-\chi\right]. \tag{B.6}$$

Combining with equation (B.5) yields:

$$X_t-W'_t+(1-s)\beta E_t\left[S^{W'}_{Nt+1}\right]=(1-\delta)\left[\frac{\kappa_0}{q(\theta_t)}+\kappa_1-\lambda_t-\chi\right]. \tag{B.7}$$

Isolating W_t' to one side of the equation:

$$\begin{aligned} W_t' &= X_t + (1-\delta)\chi + (1-s)\beta E_t\left[S_{Nt+1}^{W'}\right] - (1-\delta)\left[\frac{\kappa_0}{q(\theta_t)} + \kappa_1 - \lambda_t\right] && \text{(B.8)} \\ &= X_t + (1-\delta)\chi + (1-s)\beta E_t\left[S_{Nt+1}^{W'}\right] - (1-\delta)\beta E_t\left[S_{Nt+1}^{W}\right] && \text{(B.9)} \\ &= X_t + (1-\delta)\chi + \beta E_t\left[(1-s)S_{Nt+1}^{W'} - (1-\delta)S_{Nt+1}^{W}\right], && \text{(B.10)} \end{aligned}$$

which is identical to equation (22). Leading equation (B.6) by one period, plugging it along with equation (B.4) into equation (B.7), and solving for W_t' yield:

$$W_t' = X_t - (1-\delta)\left(\left(\frac{\kappa_0}{q(\theta_t)} + \kappa_1 - \lambda_t - \chi\right) - (1-s)\beta E_t\left[\frac{\kappa_0}{q(\theta_{t+1})} + \kappa_1 - \lambda_{t+1} - \chi\right]\right). \quad \text{(B.11)}$$

We further characterize the agreement condition (23) as follows. Rewriting equation (B.5) with W_t and combining with equation (B.4) yield $S_{Nt}^W = X_t - W_t + (1-s)\left[\kappa_0/q(\theta_t) + \kappa_1 - \lambda_t\right]$. As such, the agreement condition becomes:

$$X_t - W_t + (1-s)\left(\frac{\kappa_0}{q(\theta_t)} + \kappa_1 - \lambda_t\right) + J_{Nt}^W > J_{Ut}. \quad \text{(B.12)}$$

Although equations (22) and (23) are easier to interpret, we implement equations (B.11) and (B.12) in our numerical algorithm.

References

Andolfatto, David, 1996. Business cycles and labor-market search, *American Economic Review* 86, 112–132.

Bai, Hang, 2016, Unemployment and credit risk, working paper, University of Connecticut.

Barnichon, Regis, 2010, Building a composite help-wanted index, *Economic Letters* 109, 175–178.

Barro, Robert J., 2006, Rare disasters and asset markets in the twentieth century, *Quarterly Journal of Economics* 121, 823–866.

Barro, Robert J., and José F. Ursúa, 2008, Macroeconomic crises since 1870, *Brookings Papers on Economic Activity* 1, 255–335.

Berridge, William A., 1929, Labor turnover, *Monthly Labor Review* 29, 62–65.

Berridge, William A., 1961, Observations on Metropolitan Life's help-wanted advertising index — and "Welcome to the Conference Board!" *The Conference Board Business Record* February, 32–37.

Binmore, Ken, Ariel Rubinstein, and Asher Wolinsky, 1986, The Nash bargaining solution in economic modelling, *Rand Journal of Economics* 17, 176–188.

Bowler, Mary, and Teresa L. Morisi, 2006, Understanding the employment measures from the CPS and CES survey, *Monthly Labor Review* February, 23–38.

Chatterjee, Satyajit, and Dean Corbae, 2007, On the aggregate welfare cost of Great Depression unemployment, *Journal of Monetary Economics* 54, 1529–1544.

Cholette, Pierre A., 1984, Adjusting sub-annual series to yearly benchmarks, *Survey Methodology* 10, 35–49.

Christiano, Lawrence J., and Jonas D. M. Fisher, 2000, Algorithms for solving dynamic models with occasionally binding constraints, *Journal of Economic Dynamics and Control* 24, 1179–1232.

Cole, Harold L. and Lee E. Ohanian, 2004, New Deal policies and the persistence of the Great Depression: a general equilibrium analysis, *Journal of Political Economy* 112, 779–812.

Dagum, Estela Bee, and Pierre A. Cholette, 2006, *Benchmarking, Temporal Distribution, and Reconciliation Methods for Time Series*, Springer.

Darby, Michael R., 1976, Three-and-a-half million U.S. employees have been mislaid: Or, an explanation of unemployment, 1934–1941, *Journal of Political Economy* 84, 1–26.

Den Haan, Wouter J., Garey Ramey, and Joel Watson, 2000, Job destruction and propagation of shocks, *American Economic Review* 90, 482–498.

Denton, Frank T., 1971, Adjustment of monthly or quarterly series to annual totals: An approach based on quadratic minimization, *Journal of the American Statistical Association* 66, 99–102.

Diamond, Peter A., 1982, Wage determination and efficiency in search equilibrium, *Review of Economic Studies* 49, 217–227.

Gertler, Mark, and Antonella Trigari, 2009, Unemployment fluctuations with staggered Nash wage bargaining, *Journal of Political Economy* 117, 38–86.

Gourio, Francois, 2012, Disaster risk and business cycles, *American Economic Review* 102, 2734–2766.

Hagedorn, Marcus, and Iourii Manovskii, 2008, The cyclical behavior of equilibrium unemployment and vacancies revisited, *American Economic Review* 98, 1692–1706.

Hall, Robert E., 2005, Employment fluctuations with equilibrium wage stickiness, 2005, *American Economic Review* 95, 50–65.

Hall, Robert E., and Paul R. Milgrom, 2008, The limited influence of unemployment on the wage bargain, *American Economic Review* 98, 1653–1674.

Hamilton, James D., 2018, Why you should never use the Hodrick-Prescott filter, *Review of Economics and Statistics* 100, 831–843.

Hodrick, Robert J., and Edward C. Prescott, 1997, Postwar U.S. business cycles: An empirical investigation, *Journal of Money, Credit, and Banking* 29, 1–16.

Kendrick, John W., 1961, *Productivity Trends in the United States*, Princeton University Press.

Lebergott, Stanley, 1964, *Manpower in Economic Growth: The American Record Since 1800*, McGraw-Hill Book Company.

Macaulay, Frederick R., 1938, The movements of interest rates, bond yields, and stock prices in the United States since 1856, New York: National Bureau of Economic Research.

Merz, Monika, 1995, Search in labor market and the real business cycle, *Journal of Monetary Economics* 95, 269–300.

Miranda, Mario J., and Paul L. Fackler, 2002, *Applied Computational Economics and Finance*, The MIT Press, Cambridge, Massachusetts.

Miron, Jeffrey A., and Christina D. Romer, 1990, A new monthly index of industrial production, *Journal of Economic History* 50, 321–337.

Mortensen, Dale T., 1982, The matching process as a noncooperative bargaining game, in J. J. McCall, ed., *The Economics of Information and Uncertainty*, Chicago: University of Chicago Press, 233–254.

Mortensen, Dale T., and Éva Nagypál, 2007, More on unemployment and vacancy fluctuations, *Review of Economic Dynamics* 10, 327–347.

Ohanian, Lee E., 2009, What—or who—started the great depression, *Journal of Economic Theory* 144, 2310–2335.

Petrosky-Nadeau, Nicolas, and Etienne Wasmer, 2013, The cyclical volatility of labor markets under frictional financial market, *American Economic Journal: Macroeconomics* 5, 193–221.

Petrosky-Nadeau, Nicolas, and Lu Zhang, 2017, Solving the Diamond-Mortensen-Pissarides model accurately, *Quantitative Economics* 8, 611–650.

Petrosky-Nadeau, Nicolas, Lu Zhang, and Lars-Alexander Kuehn, 2018, Endogenous disasters, *American Economic Review* 108, 2212–2245.

Pissarides, Christopher A., 1985, Short-run dynamics of unemployment, vacancies, and real wages, *American Economic Review* 75, 676–690.

Pissarides, Christopher A., 2009, The unemployment volatility puzzle: Is wage stickiness the answer? *Econometrica* 77, 1339–1369.

Preston, Noreen L., 1977, *The Help-wanted Index: Technical Description and Behavioral Trends*, New York: Conference Board.

Quilis, Enrique M., 2013, A Matlab library of temporal disaggregation and interpolation methods, working paper, Ministry of Economy and Competitiveness, Spain.

Ravn, Morten O., and Harald Uhlig, 2002, On adjusting the Hodrick-Prescott filter for the frequency of observations, *Review of Economics and Statistics* 84, 371–380.

Rietz, Thomas A., 1988, The equity risk premium: A solution, *Journal of Monetary Economics* 22, 117–131.

Rouwenhorst, K. Geert, 1995, Asset pricing implications of equilibrium business cycle models, in T. Cooley ed., *Frontiers of Business Cycle Research*, Princeton: Princeton University Press, 294–330.

Shimer, Robert, 2005, The cyclical behavior of equilibrium unemployment and vacancies, *American Economic Review* 95, 25–49.

Weir, David R., 1992, A century of U.S. unemployment, 1890–1990: Revised estimates and evidence for stabilization, In *Research in Economic History*, edited by Roger L. Ransom, 301–346, JAI Press.

Zagorsky, Jay L., 1998, Job vacancies in the United States: 1923 to 1994, *Review of Economics and Statisitics* 80, 338–345.

Table 1 : Second Moments of the Labor Market in the Data

The civilian unemployment rates, U, the vacancy rates, V, and the labor productivity, X, are converted to quarterly averages of monthly series. The labor market tightness is then calculated as $\theta = V/U$. In Panel A, the U and X series are from January 1890 to December 2017, and the V and θ series are from January 1919 onward. The correlations involving V and θ are based on the sample after January 1919. Otherwise, the correlations are from the sample starting from January 1890. In Panel B, all the moments are from the post-1951 sample. All the variables are in log deviations from the HP-trend with a smoothing parameter of 1,600.

		U	V	θ	X	U	V	θ	X
		Panel A: 1890:1–2017:12				Panel B: 1951:1–2017:12			
Standard deviation		0.258	0.172	0.379	0.039	0.126	0.135	0.256	0.012
Autocorrelation		0.904	0.896	0.912	0.588	0.889	0.905	0.905	0.758
Correlation matrix	U		−0.791	−0.961	−0.383		−0.922	−0.979	−0.222
	V			0.930	0.301			0.982	0.394
	θ				0.367				0.317

Table 2 : Estimated Aggregate State Transition Probabilities and Unconditional Probabilities of the Three Good, Bad, and Crisis States, January 1890–December 2017, 1536 Months

The state transition matrix is given in equation (1), the transition probabilities in equation (2), and the standard errors (in parentheses) in equation (3). The unconditional probabilities of the states in the last row are calculated by raising the transition matrix to the power 1,000. All the probabilities and their standard errors are in percent. The good state is identified as months in which the unemployment rates, U, are below the median in the sample, the bad state as months in which the U values are above or equal to the median but below the crisis cutoff rate of 15%, and the crisis state as months in which the U values are above or equal to the crisis cutoff rate.

	Good	Bad	Crisis	Good	Bad	Crisis
	Civilian unemployment rates			Private nonfarm unemployment rates		
Good	95.96	4.04	0	96.09	3.91	0
	(0.71)	(0.71)	(0)	(0.70)	(0.70)	(0)
Bad	4.29	95.16	0.55	4.86	94.00	1.13
	(0.75)	(0.80)	(0.28)	(0.87)	(0.96)	(0.43)
Crisis	0	8.89	91.11	0	4.64	95.36
	(0)	(4.24)	(4.24)	(0)	(1.71)	(1.71)
Unconditional probabilities	49.97	47.10	2.93	49.97	40.20	9.84

Table 3 : The Benchmark Monthly Calibration

β is the time discount factor, ρ the persistence of log labor productivity, σ its conditional volatility, s the separation rate, ι the elasticity of the matching function, b the flow value of unemployment activities, δ the probability of breakdown in bargaining, χ the employer's cost of delaying in bargaining, κ_0 the proportional cost, and κ_1 the fixed cost of vacancy posting.

β	ρ	σ	s	ι	b	δ	χ	κ_0	κ_1
$0.99^{1/3}$	$0.95^{1/3}$	0.00635	0.035	1.25	0.71	0.1	0.25	0.2	0.35

Table 4 : The Aggregate State Transition Matrix and Unconditional Probabilities of the Three Economic States in the Model

From the model's stationary distribution, we simulate 25,000 artificial samples, each with 1,536 months. We split the samples into two groups, non-crisis samples (in which the maximum unemployment rate is less than 15%) and crisis samples (in which the maximum rate is greater than or equal to 15%). On each crisis sample, we calculate the state transition matrix and unconditional probabilities of the states as in Table 2. We report the cross-simulation averages and standard deviations in parentheses, both of which are in percent, across the crisis samples.

	Good	Bad	Crisis
Good	97.93	2.07	0
	(0.6)	(0.6)	(0)
Bad	2.29	97.18	0.53
	(0.66)	(0.79)	(0.38)
Crisis	0	8.2	91.8
	(0)	(10.22)	(10.24)
Unconditional probability	49.92	45.31	4.77
	(1,77)	(4.01)	(4.31)

Table 5 : Second Moments of the Labor Market in the Model

We simulate 25,000 artificial samples from the model, each with 1,536 months. We split the samples into two groups, non-crisis samples (in which the maximum unemployment rate is less than 15%) and crisis samples (in which the maximum rate is greater than or equal to 15%). We implement the same empirical procedure as in Table 1 and report cross-simulation averages and standard deviations (in parentheses) conditionally on the non-crisis samples and on the crisis samples.

		U	V	θ	X	U	V	θ	X
		Panel A: Non-crisis samples				Panel B: Crisis samples			
Volatility		0.126	0.168	0.270	0.013	0.156	0.182	0.303	0.013
		(0.023)	(0.017)	(0.034)	(0.001)	(0.020)	(0.013)	(0.028)	(0.001)
Persistence		0.813	0.615	0.765	0.771	0.845	0.600	0.780	0.782
		(0.034)	(0.063)	(0.038)	(0.035)	(0.022)	(0.044)	(0.026)	(0.024)
Correlation	U		−0.681	−0.890	−0.824		−0.599	−0.876	−0.815
			(0.057)	(0.019)	(0.036)		(0.050)	(0.016)	(0.027)
	V			0.939	0.939			0.911	0.913
				(0.017)	(0.016)			(0.016)	(0.016)
	θ				0.969				0.971
					(0.011)				(0.010)

Table 6 : Comparative Statics, Aggregate State Transition Matrix and Unconditional Probabilities of the Three Economic States in the Model

This table reports six comparative static experiments: (i) the probability of breakdown in bargaining $\delta = 0.15$; (ii) the delaying cost $\chi = 0.2$; (iii) the proportional cost of vacancy $\kappa_0 = 0.15$; (iv) the fixed cost of vacancy $\kappa_1 = 0.3$; (v) the separation rate $s = 0.04$; and (vi) the curvature parameter of the matching function $\iota = 0.9$. In each experiment, all the other parameters remain identical to those in the benchmark calibration. For each experiment, we simulate 25,000 artificial samples (each with 1,536 months) from the model's stationary distribution. We split the samples into two groups: non-crisis samples (in which the maximum unemployment rate is less than 15%) and crisis samples (in which the maximum rate is greater than or equal to 15%). On each crisis sample, we calculate the state transition matrix and unconditional probabilities of the states per the procedure in Table 2 and report cross-simulation averages, all in percent.

	Good	Bad	Crisis	Good	Bad	Crisis
	Panel A: $\delta = 0.15$			Panel B: $\chi = 0.2$		
Good	97.98	2.02	0	98.01	1.99	0
Bad	2.08	97.7	0.22	2.02	97.8	0.17
Crisis	0	17.64	82.3	0	21.55	78.41
Unconditional probability	49.85	48.36	1.76	49.78	48.89	1.31
	Panel C: $\kappa_0 = 0.15$			Panel D: $\kappa_1 = 0.3$		
Good	97.93	2.07	0	97.93	2.07	0
Bad	2.24	97.29	0.47	2.24	97.27	0.49
Crisis	0	11.42	88.58	0	10.92	89.07
Unconditional probability	49.89	46.32	3.79	49.89	46.17	3.94
	Panel E: $s = 0.04$			Panel F: $\iota = 0.9$		
Good	97.91	2.09	0	97.94	2.06	0
Bad	2.65	96.08	1.27	2.33	97.16	0.51
Crisis	0	6.22	93.78	0	5.6	94.39
Unconditional probability	49.98	40.05	9.97	49.9	44.32	5.78

Table 7 : Comparative Statics, Second Moments in the Labor Market in Normal Periods

This table reports six comparative static experiments: (i) the probability of breakdown in bargaining $\delta = 0.15$; (ii) the delaying cost $\chi = 0.2$; (iii) the proportional cost of vacancy $\kappa_0 = 0.15$; (iv) the fixed cost of vacancy $\kappa_1 = 0.3$; (v) the separation rate $s = 0.04$; and (vi) the curvature parameter of the matching function $\iota = 0.9$. In each experiment, all the other parameters remain identical to those in the benchmark calibration. For each experiment, we simulate 25,000 artificial samples (each with 1,536 months) from the model's stationary distribution. We split the samples into two groups: non-crisis samples (in which the maximum unemployment rate is less than 15%) and crisis samples (in which the maximum rate is greater than or equal to 15%). On each non-crisis sample, we implement the same procedure as in Table 1 and report the cross-simulation averages.

	U	V	θ	X		U	V	θ	X
	Panel A: $\delta = 0.15$					Panel B: $\chi = 0.2$			
Volatility	0.1	0.132	0.214	0.013		0.068	0.137	0.195	0.013
Persistence	0.819	0.625	0.772	0.774		0.79	0.698	0.769	0.776
Correlation		−0.705	−0.9	−0.859	U		−0.776	−0.896	−0.777
			0.943	0.948	V			0.974	0.96
				0.984	θ				0.947
	Panel C: $\kappa_0 = 0.15$					Panel D: $\kappa_1 = 0.3$			
Volatility	0.119	0.187	0.284	0.013		0.114	0.163	0.257	0.013
Persistence	0.801	0.652	0.764	0.772		0.806	0.63	0.764	0.771
Correlation		−0.712	−0.886	−0.793	U		−0.703	−0.892	−0.814
			0.955	0.952	V			0.948	0.945
				0.959	θ				0.964
	Panel E: $s = 0.04$					Panel F: $\iota = 0.9$			
Volatility	0.117	0.163	0.259	0.013		0.108	0.153	0.24	0.013
Persistence	0.804	0.614	0.759	0.767		0.831	0.604	0.765	0.769
Correlation		−0.706	−0.896	−0.832	U		−0.685	−0.886	−0.852
			0.947	0.945	V			0.945	0.937
				0.97	θ				0.98

Figure 1 : U.S. Monthly Civilian Unemployment Rates and Private Nonfarm Unemployment Rates, January 1890–December 2017, 1,536 Months

The blue solid line depicts civilian unemployment rates, and the red broken line private nonfarm unemployment rates. Both unemployment rates are in percent (%).

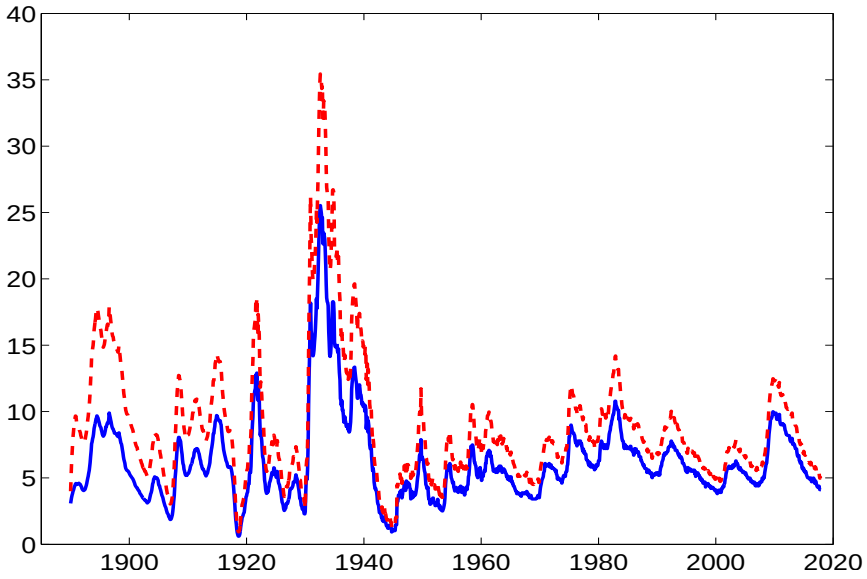

Figure 2 : U.S. Monthly Job Openings, Civilian Labor Force, Vacancy Rates, and Labor Market Tightness, January 1919–December 2017, 1,188 Months

The labor market tightness is the ratio of the vacancy rates over civilian unemployment rates.

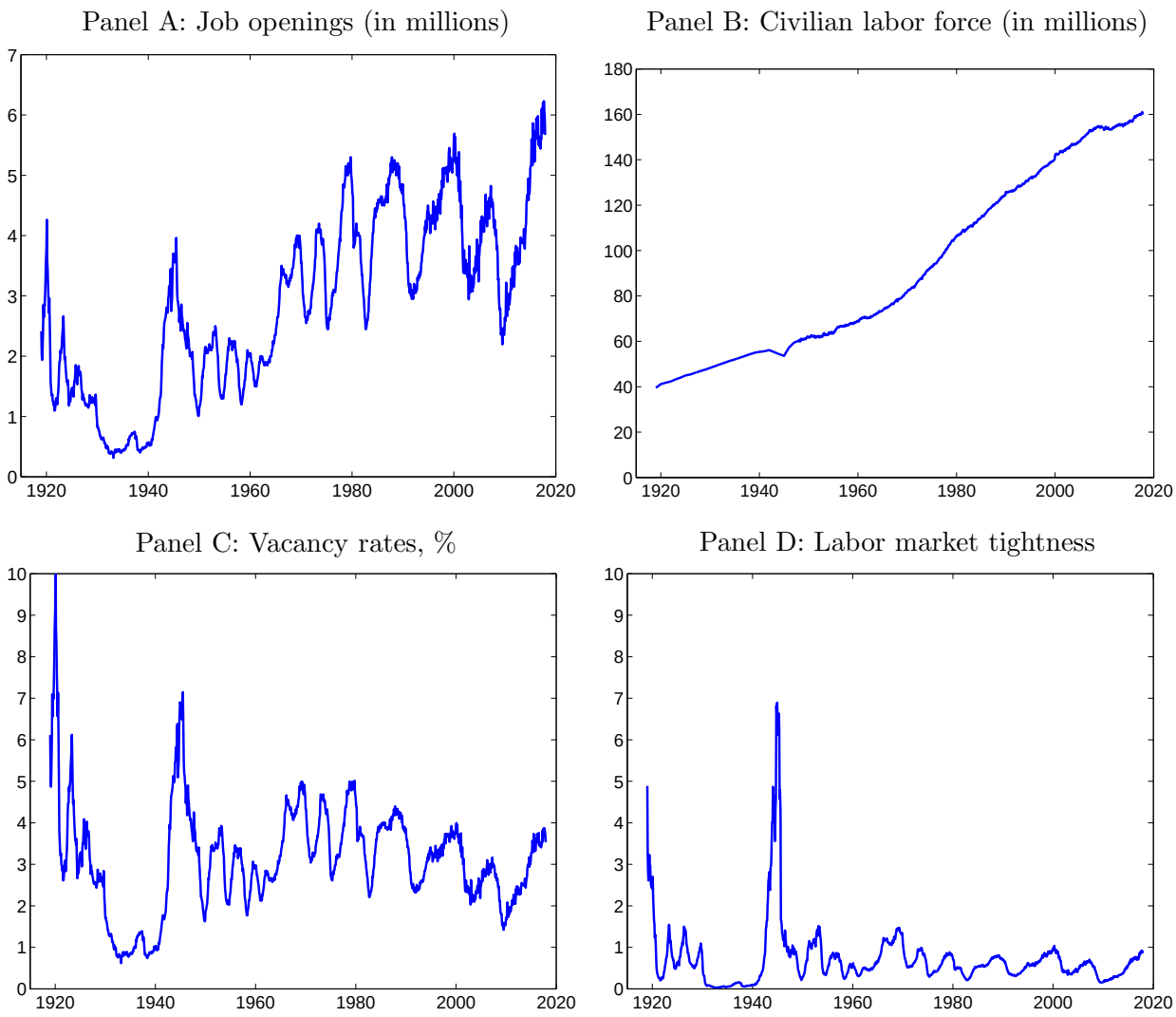

Figure 3 : The US Beveridge Curve, January 1919–December 2017, 1,188 Months

The Beveridge curve is the scatter plot of vacancy rates versus civilian unemployment rates.

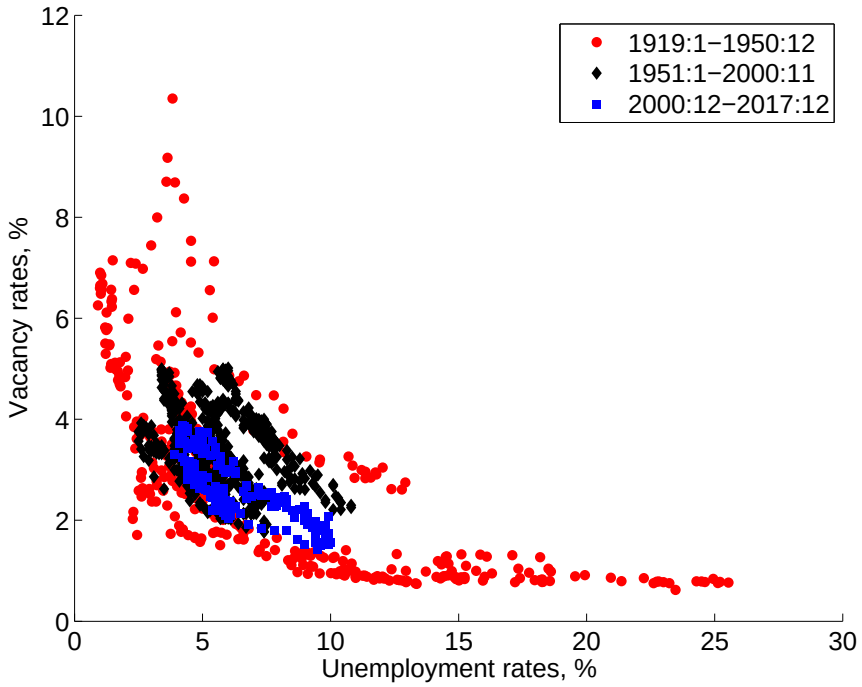

Figure 4 : U.S. Monthly Nonfarm Business Real Output, Private Nonfarm Employment, and Labor Productivity (Real Output per Person), January 1890–December 2017, 1,536 Months

Nonfarm business real output is an index with the value of 100 for the base year (2012). The unit of private nonfarm employment is number in millions. Labor productivity is an index with the value of 100 for the base year (2012).

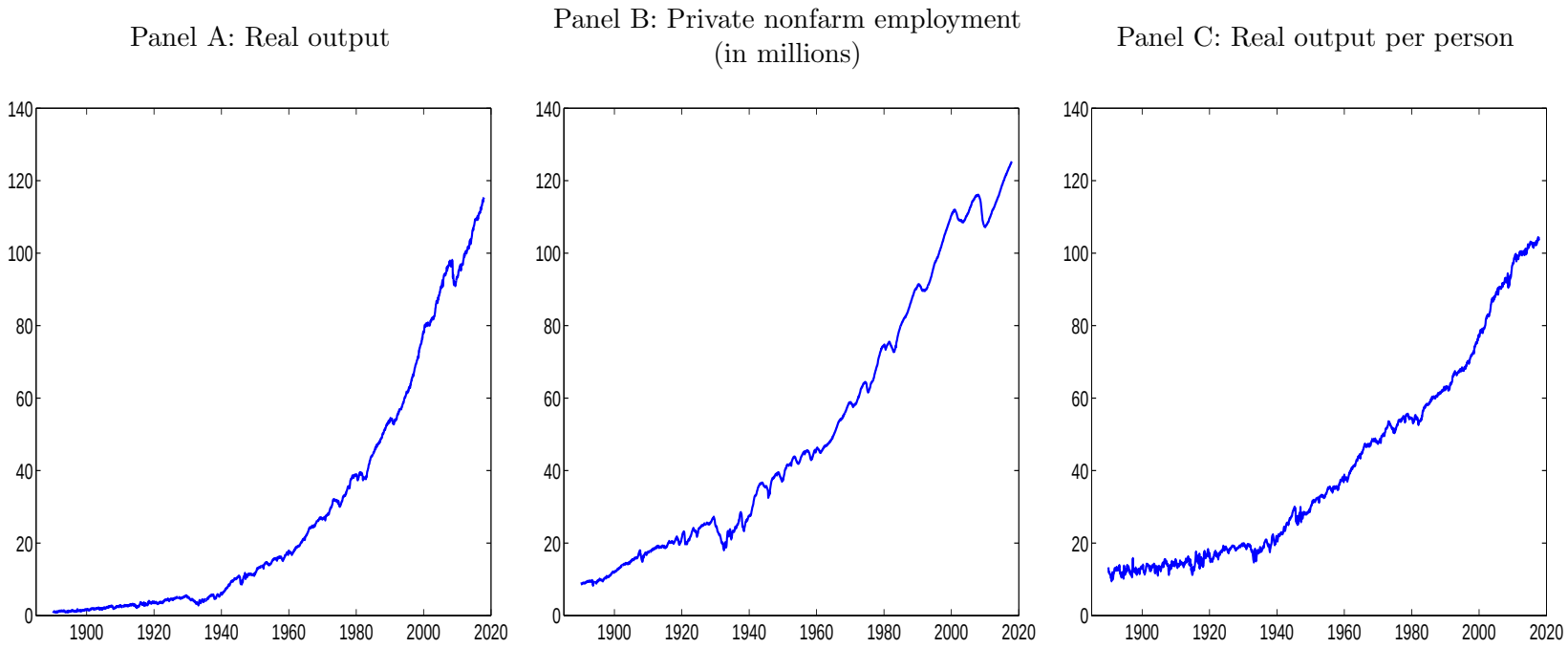

Figure 5 : Key Variables in the Model's Competitive Equilibrium

We plot against the log labor productivity, x_t, the model's key variables including the conditional expectation, $\mathcal{E}_t$, in equation (25); the labor market rightness, θ_t; the vacancy filling rate, $q(\theta_t)$; the job finding rate, $f(\theta_t)$; the equilibrium wage, W_t; and the wage offered by the workers, W_t'.

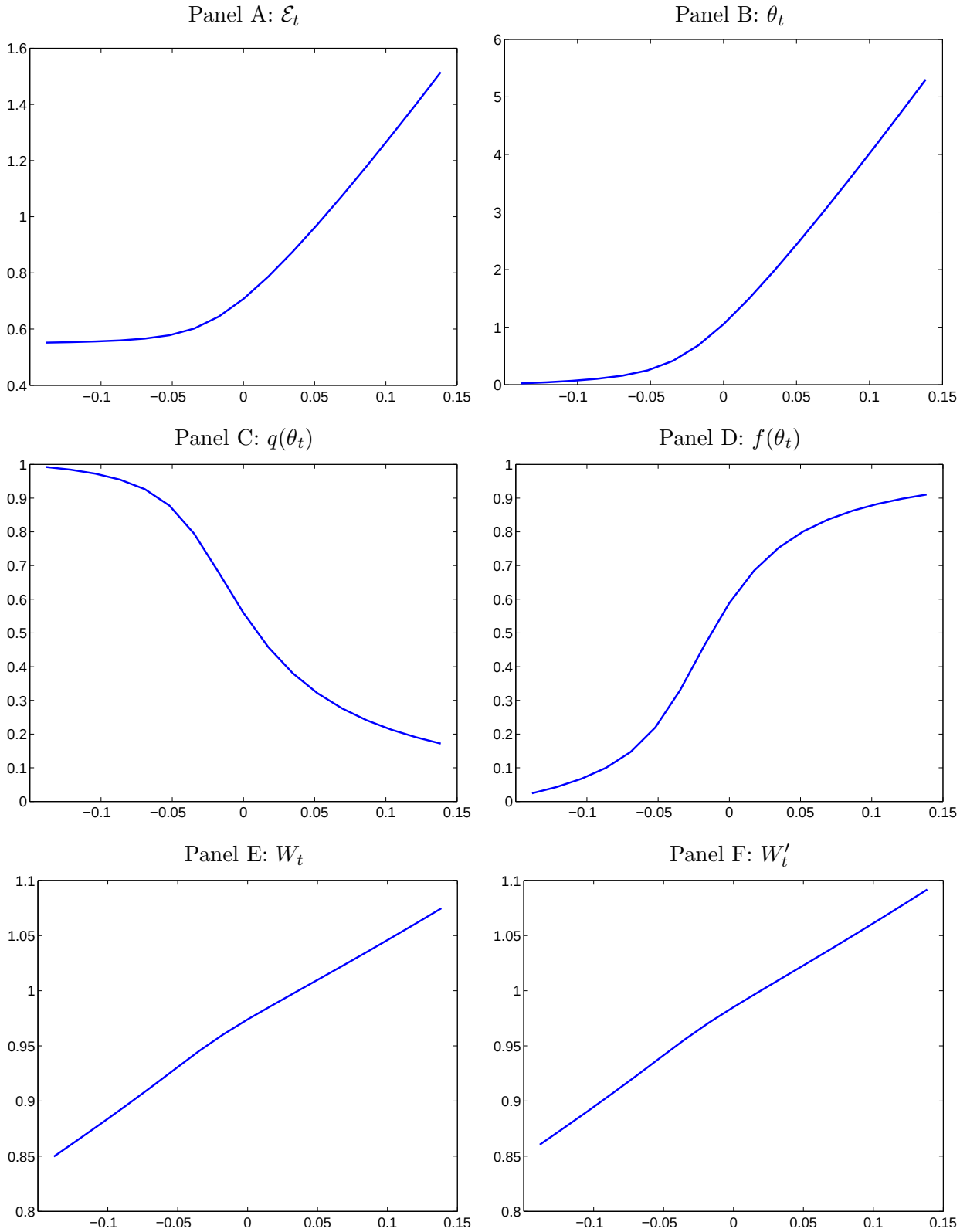

Figure 6 : The Unemployment-log productivity Relation, the Vacancy-log productivity Relation, and Empirical Cumulative Distribution Functions (C.d.f.) of Unemployment and Vacancy Rates

Results are based on the one-million-month simulated data from the model's stationary distribution. The unemployment and vacancy rates are in percent.

Panel A: Unemployment vs. log productivity

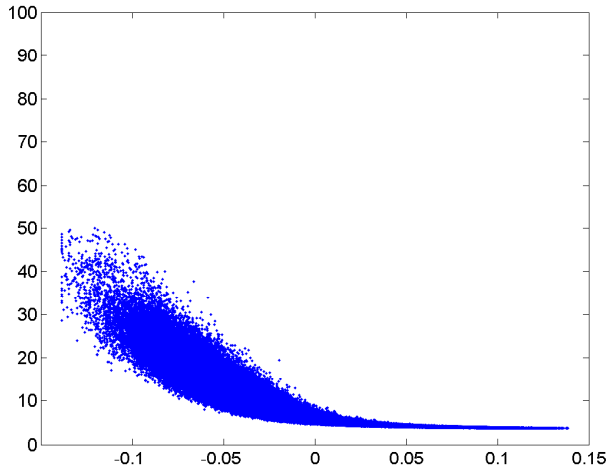

Panel B: Vacancy vs. log productivity

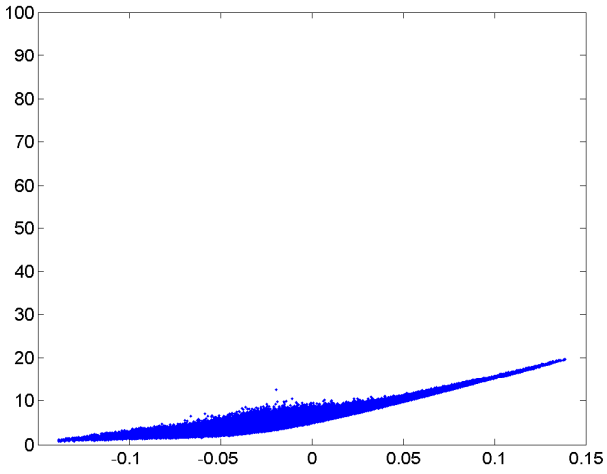

Panel C: C.d.f. of unemployment

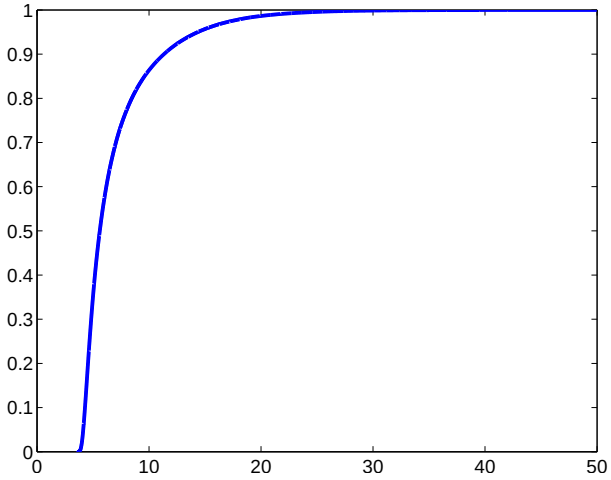

Panel D: C.d.f. of vacancy

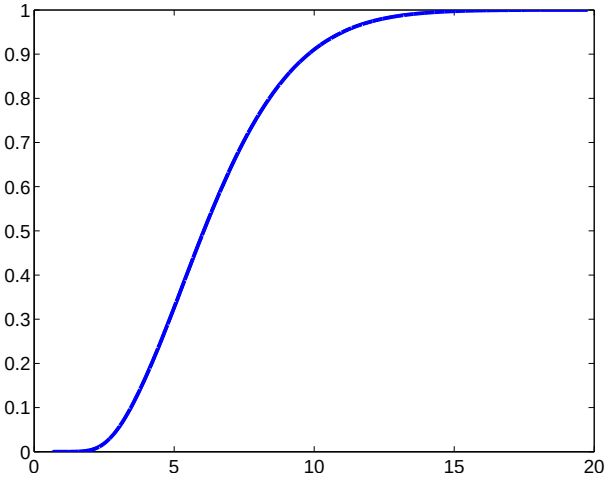

Figure 7 : Nonlinear Impulse Response Functions

The impulse responses are from three different initial points: the 5, 50, and 95 percentiles of the model's bivariate distribution of employment and log productivity, respectively. The responses in wages and labor market tightness are in percentage deviations from the values at a given initial point, and the responses in unemployment are in levels (times 100). We average the impulse responses across 25,000 simulations, each of which has 120 months. The blue solid (red broken) lines are the responses to a positive (negative) one-standard-deviation shock to log productivity.

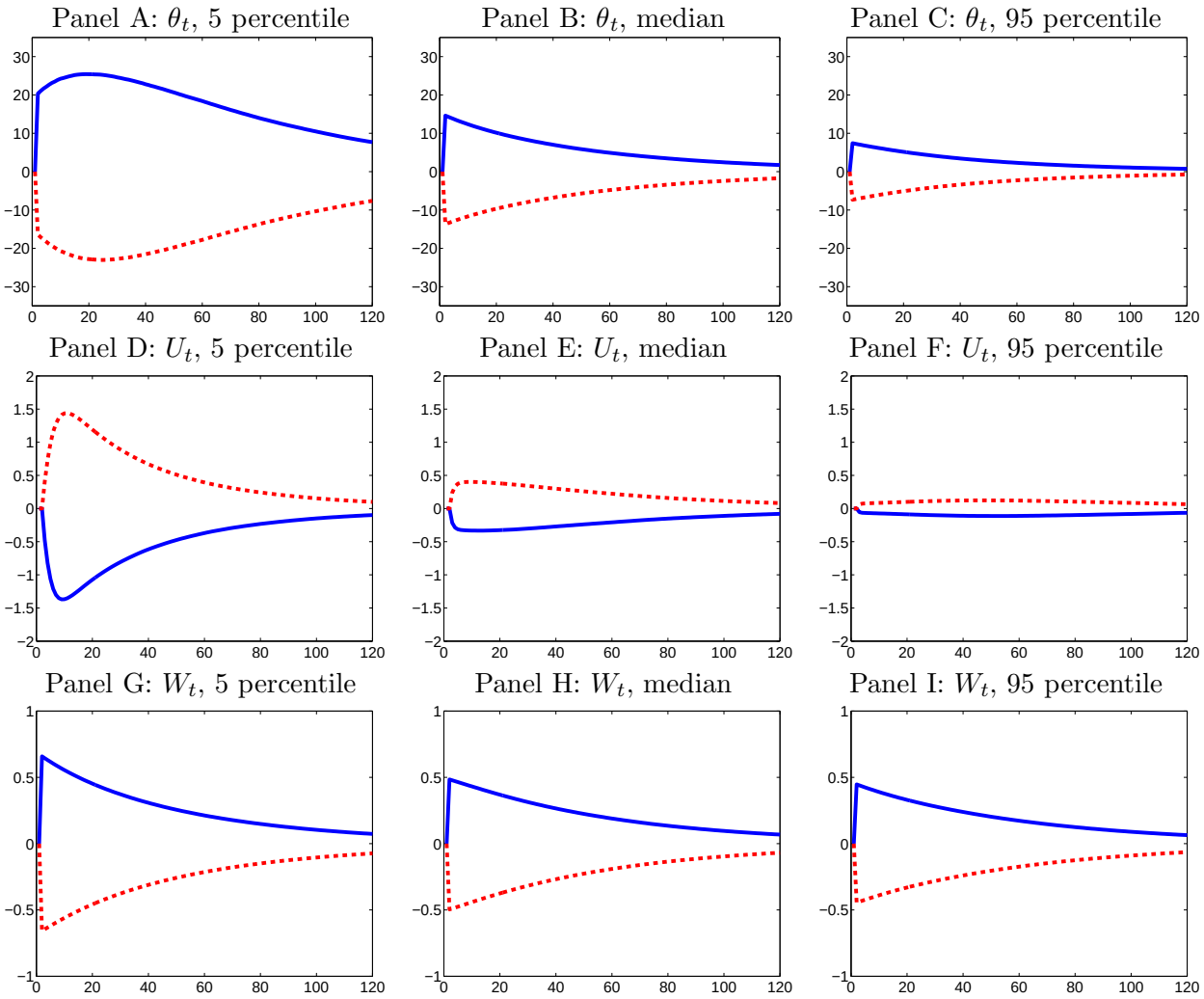

Figure 8 : Accounting for the Great Depression, January 1929–December 1939

Panel A plots the monthly log labor productivity in the data detrended with the Hamilton (2018) method by regressing the 12-month ahead values of the log productivity on its current, one-, two-, three-, ..., and 11-month-lagged values. The cyclical component is the residual from the regression. We feed this cyclical component of the log productivity into the model to calculate its implied output, unemployment, and labor market tightness series, which are plotted in the blue solid lines in Panels B, C, and D, respectively. The red broken lines are the detrended real output in the data via the Hamilton method in Panel B, civilian unemployment rates in Panel C, and the market tightness in Panel D. The black dotted line in Panel C is private nonfarm unemployment rates.